Georgia State University
ScholarWorks @ Georgia State University

Geosciences Theses | Department of Geosciences

Fall 12-16-2015

Assessing the Effectiveness of Extensive Green Roofs at Improving Environmental Conditions in Atlanta, Georgia

Sharon Murphy

Follow this and additional works at: https://scholarworks.gsu.edu/geosciences_theses

Recommended Citation
Murphy, Sharon, "Assessing the Effectiveness of Extensive Green Roofs at Improving Environmental Conditions in Atlanta, Georgia." Thesis, Georgia State University, 2015.
https://scholarworks.gsu.edu/geosciences_theses/87

This Thesis is brought to you for free and open access by the Department of Geosciences at ScholarWorks @ Georgia State University. It has been accepted for inclusion in Geosciences Theses by an authorized administrator of ScholarWorks @ Georgia State University. For more information, please contact scholarworks@gsu.edu.

ASSESSING THE EFFECTIVENESS OF EXTENSIVE GREEN ROOFS AT IMPROVING ENVIRONMENTAL CONDITIONS IN ATLANTA, GEORGIA

by

SHARON MURPHY

Under the Direction of Dr. Jeremy Diem, PhD.

ABSTRACT

Green roofs can be an effective mitigation strategy to offset the environmental impact that urbanization has on the environment. The roof area for the city of Atlanta and for the Georgia State University campus was used to compare the effectiveness of green roofs at removing pollutants, abating stormwater runoff, and reducing the urban heat island at different scales. Results show that the warmest part of the city is the urban core with a mean of 33.5°C, which is also the area of the city with the highest percentage of impermeable surfaces at 91%. At the GSU scale, green roofs can reduce land surface temperature in the urban core up to 2.62°C, remove up to 73 kg of atmospheric pollutants annually, and reduce stormwater runoff by up to 32.3% annually. Results were less significant at the Atlanta scale due to the large amount of vegetated surfaces that already exist.

INDEX WORDS: Urban Heat Island, Green Roof, Land Surface Temperature, Atlanta Temperature, Climate Change Atlanta, Extreme Heat Events Atlanta, Stormwater Runoff, Pollutants, Atlanta, NO_2, SO_2, PM_{10}, O_3. Atmospheric Pollutants,

ASSESSING THE EFFECTIVENESS OF EXTENSIVE GREEN ROOFS AT IMPROVING ENVIRONMENTAL CONDITIONS IN ATLANTA, GEORGIA

by

SHARON MURPHY

A Thesis Submitted in Partial Fulfillment of the Requirements for the Degree of

Master of Science

In the College of Arts and Sciences

Georgia State University

2015

Copyright by
Sharon L. Murphy
2015

ASSESSING THE EFFECTIVENESS OF EXTENSIVE GREEN ROOFS AT IMPROVING ENVIRONMENTAL CONDITIONS IN ATLANTA, GEORGIA

by

SHARON MURPHY

Committee Chair: Jeremy Diem

Committee: Brian Meyer

Daijun Dai

Electronic Version Approved:

Office of Graduate Studies

College of Arts and Sciences

Georgia State University

December 2015

DEDICATION

This work is dedicated to my children Kristen, Taylor, and Ryan and hopefully serves as an inspiration to them as they navigate the journey of life. You are never too old to pursue your dreams, and don't ever let anyone tell you that you are not capable of achieving those dreams. It is also dedicated to the professors and staff of the Department of Geosciences at GSU who have challenged me and believed in me at times when I didn't believe in myself.

ACKNOWLEDGEMENTS

Special thanks to Dr. Jeremy Diem for inspiring me to reach for the fruit at the top of the tree instead of settling for the low hanging fruit. His guidance and good humor were essential elements to the completion of this manuscript. And lastly, a special thanks to Dr. Mark Becker for believing in me and for setting the standard for hard work and excellence that I strive to emulate in all aspects of my life.

TABLE OF CONTENTS

LIST OF TABLES

LIST OF FIGURES

1 INTRODUCTION

1.1 Background

Despite the strides made in reducing the impacts of urbanization on the environment in major cities across the globe, stormwater runoff and the urban heat island effect are increasingly becoming the leading environmental threats facing urban populations. Studies have shown that ambient air temperatures in urban areas will increase at a faster rate than the nearby rural areas due to climate change (Pompeii & Hawkins, 2011), increasing the risk of heat related mortality for urban residents (Saha, Davis, & Hondula, 2014). The high percentage of impervious surfaces associated with urbanization have caused stormwater runoff to frequently overwhelmed the sewer systems designed for much lower flow capacities, causing sewage overflows into streams and creeks that often run through neighborhoods (Zhang et al., 2015). High urban ambient air pollution has been linked to a variety of negative health outcomes such as reduced cognition in children (Calderón-Garcidueñas & Torres-Jardón, 2012), adult onset asthma (Jacquemin et al., 2015), as well as depression (Calderón-Garcidueñas et al., 2015). The Clean Air Act (CCA) of 1970 was an effort to reduce ambient air pollution in the United States, none the less, Atlanta, Georgia struggles to control ambient air pollution due to the rapid and sprawling nature of the city's growth (Goldberg, 1998). Thirty four years after the passage of the CCA a correlation between low birth weight babies and ambient air pollution still existed in Atlanta (Darrow, Klein, Strickland, Mulholland, & Tolbert, 2011). Often, the populations most at risk of poor health outcomes due to exposure to ambient air pollution also reside in the areas of the city that are also the hottest due to the urban heat island effect (Johnson & Wilson, 2009).

The urban heat island (UHI) phenomenon is defined as an increase of surface temperatures in urban settings above the surface temperatures of the surrounding rural areas (Huang, Zhou,

& Cadenasso, 2011) and this phenomenon exacerbates extreme heat events (EHE). A combination of factors including the amount of vegetation present in any given area, antecedent soil moisture, synoptic atmospheric conditions, the materials that the built environment is constructed from, as well as the size and scale of the built environment, all contribute to produce a UHI that contains elevated and spatially diverse temperatures (Johnson & Wilson, 2009). The frequency and amplitude of EHEs is expected to increase due to climate change, putting already vulnerable populations such as the elderly and the poor at an even greater risk of heat related mortality (Davis, Knappenberger, Michaels, & Novicoff, 2003). The major environmental benefits of having green roofs on buildings in urban areas is their potential to help mitigate the urban heat island (Lilliana et al, 2013), reduce ambient air pollution and stormwater runoff (Rowe, 2011), and potentially reduce the mortality rate in urban areas during an extreme heat event (Johnson & Wilson, 2009).

It is important to understand the effects of green roofs on the urban environment of humid sub-tropical cities because it is predicted that with climate change, the humid sub-tropical climate will grow to encompass most of the northeastern and Midwestern U.S. by the end of the century.

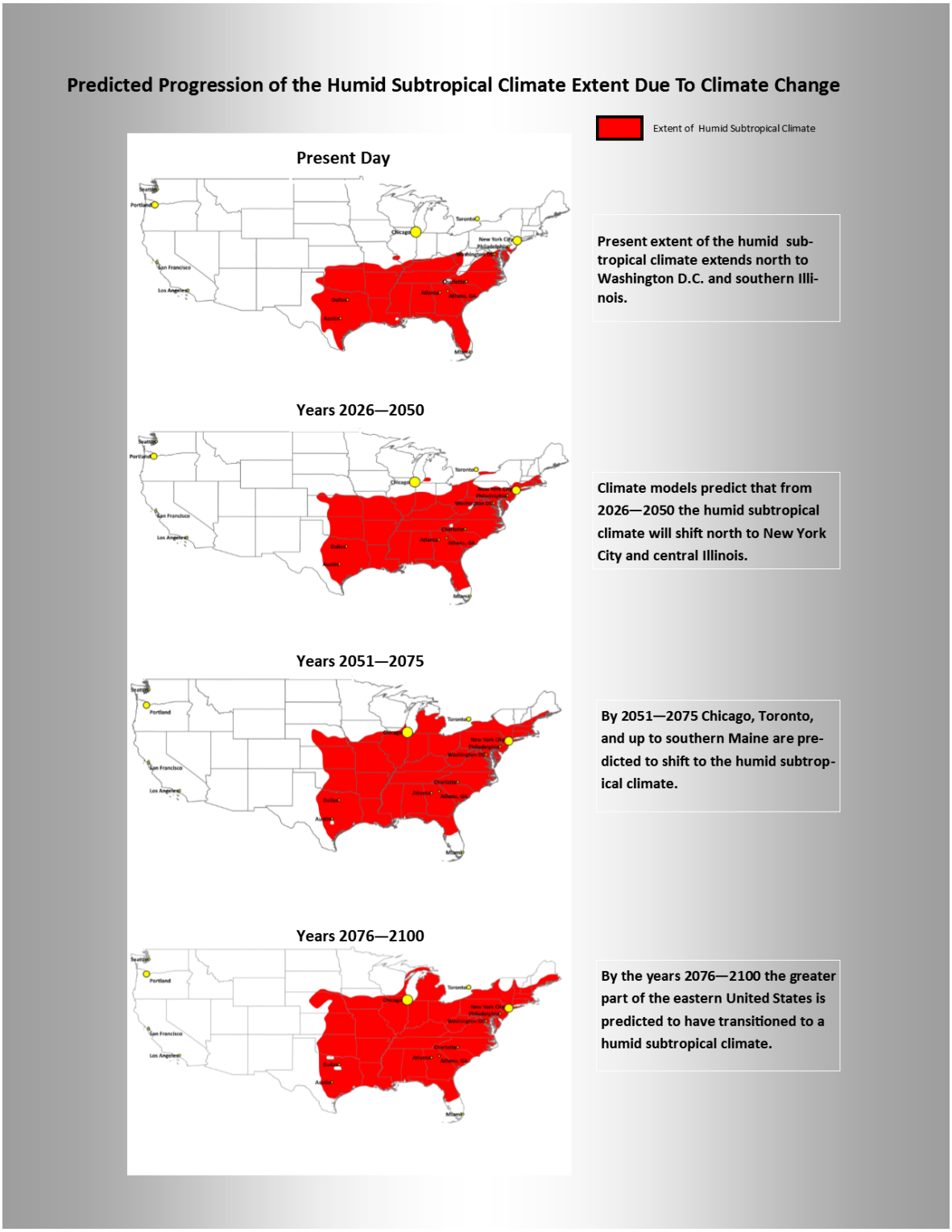

Figure 1 ThePredicted Progression of the Humid Sub-Tropical Climate

1.2 Green Roofs

A green roof is a vegetated layer that is grown on a building roof with the intention of replacing that part of the natural landscape that was destroyed when the building was constructed. They typically fall into two classification schemes: extensive or intensive, based on the depth of growing medium used. An extensive green roof consists of a shallow growing medium of three to six inches and is capable of supporting shallow rooted and short plants such as sedums and small grasses. An Intensive green roof consists of growing medium greater than six inches and can support a wider variety of vegetation such as shrubs, trees, and vegetables (U.S. Environmental Protection Agency Office of Atmospheric Programs, 2008). How effective a green roof is at mimicking a naturally vegetated space depends on several factors: the depth of the growing medium, the type of plants growing on the roof, synoptic climate conditions, and the degree of moisture present in the growing medium (Santamouris, 2014). These variables make it difficult to extrapolate the results of green roof studies from one region of the U.S. to another.

Adding greenspace at ground level in an urban setting may be impossible, so taking advantage of the real estate afforded on commercial roofs to increase greenspace is a key strategy for UHI mitigation. Urban areas have a smaller temperature differential between daytime and evening when compared to rural or suburban areas due to the inefficient cooling of the built environment at night (Buyantuyev, 2009). The albedo (a measure of reflectance) of a surface has a strong influence on the primary drivers that regulate surface temperature: the atmospheric boundary layer, emissivity, surface roughness, evaporation, and the heat capacity of an object. Vegetation has a low heat capacity and increases surface roughness, evaporation, and emissivity; all characteristics that reduce surface temperature (Fernando, 2001). Through these mechanisms, green roofs can help mitigate urban heat islands with taller buildings experiencing greater cooling load decreases, and the greatest reduction in cooling occurring on the hottest

summer days (Perini, 2014). While green roofs can produce cooling effects top to bottom, these effects are most pronounced inside the building the roof sits on and are negligible for pedestrians at ground level (Peng, 2012) (Lilliana, 2013). However, the aggregated cooling extents of urban greenspaces has been shown to be an effective mechanism for reducing the urban heat island (Dugord, 2014). A reduction of 1-3°C in the urban heat island effect was found when a combination of cool and extensive green roofs were modeled for urban areas throughout southern California, although the heating effects generated by transportation systems was not included in the model used to estimate near surface temperature changes (Georgescu, 2015) (Akbari, Pomerantz, & Taha, 2001).

Green roofs can lower surface temperatures directly through the mechanisms mentioned in the preceding paragraph, and also indirectly through a reduction of heat producing processes that occur during the production of cool air inside buildings. Direct effects can be measured and felt immediately while indirect effects may not be quantified until a green roof has been established for some time and are often difficult to account for (Akbari, 2001). While it is impossible to quantify the benefit of reducing mortality from an extreme heat event, it is possible to quantify other indirect costs associated with the reduction of air pollution, energy costs, and stormwater runoff utilizing a Net Present Value analysis (Clark, Adriaens, & Talbot, 2008). Quantifying both direct and indirect costs is an essential part of valuating the benefits of green roofs as together they have the potential to inform and guide policy decisions (Farrugia, Hudson, & McCulloch, 2013). When both direct and indirect effects are quantified, the costs associated with installing and maintaining a green roof are recovered within 14 – 20 years depending on the number of cooling and heating degree days, with warmer regions experiencing greater savings for an equal number of cooling days as a moderate climate (Thevenard, 2011). Thus removing

one of the largest barriers to widespread adoption of green roof technology (Clark, Adriaens, & Talbot, 2008).

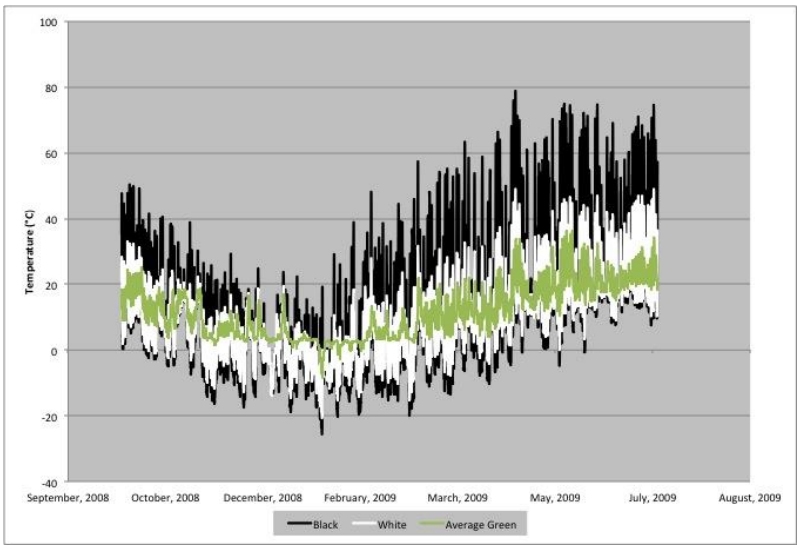

Figure 2 Comparitive Analysis of Radiative Heat Flux of Green Roofs Versus White Roofs Versus Conventional Roofs (Gaffin, Rosenzweig, Eichenbaum-Pikser, Khanbilvardi, & Susca, 2010).

1.2.1 The Influence of Green Roofs on the Urban Heat Island

Urban Heat Island (UHI) is a term that refers to the increased surface temperatures that the urban built environment causes relative to the surrounding rural area. Urban environments generally have reduced vegetative land cover, an increase in impervious surfaces, and consist of a built environment that creates urban canyons, all of which contribute to increased surface temperatures, especially at night (Targino, Krecl, & Coraiola, 2014). Loss of vegetative land cover reduces environmental cooling via evapotranspiration and also reduces surface albedo causing an increase in heat absorption (Coseo & Larsen, 2014). The tall buildings characteristic of an urban center have been shown to be the primary factor in the creation of the UHI (Heisler & Brazel, 2010) because the thermal properties of the building materials used in urban built environments change the radiative flux through heat absorption during the day and radiant heat at night (Huang, Zhou, & Cadenasso, 2011). These factors raise the minimum daily temperature (nighttime temperature) within the urban boundary, and it is the amplitude of the minimum daily

temperature that has been linked to an increase in mortality during an EHE (Luber & McGeehin, 2008). The more heat the UHI absorbs and stores during the day, the more heat the UHI radiates at night in the form of infrared radiation, latent heat flux, and sensible heat flux, raising nighttime temperatures, human discomfort, and increasing the potential for heat related mortality among urban residents (Luber & McGeehin, 2008, Alexander, 2011).

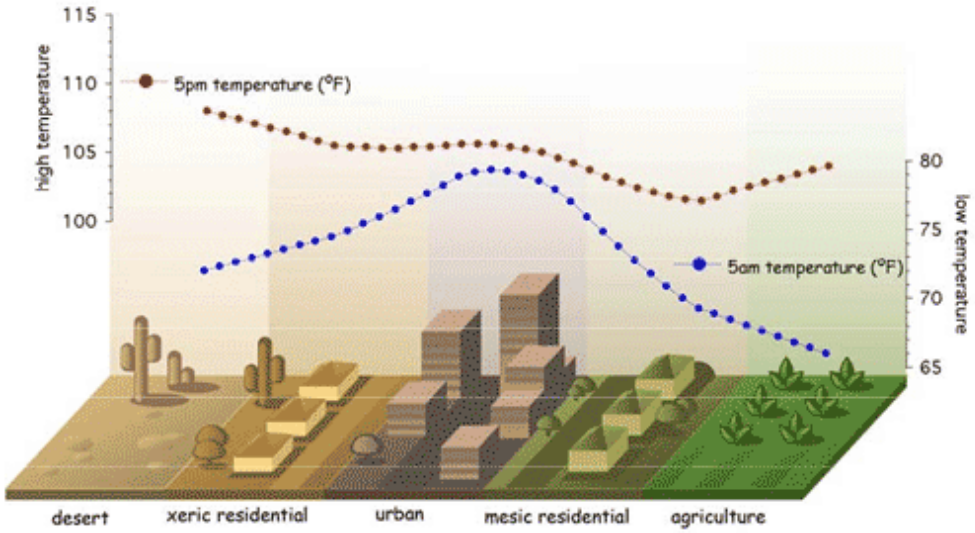

Figure 3 This graphic demonstrates the effect that the urban built environment has on the diurnal temperature range. The 5am temperature over the urban area remains elevated. Figure courtesy of the Minnesota Department of Health.

Due to climate change, the UHI effect is expected to become more severe. Prior to 1930 there were few positive trends associated with minimum and maximum temperature extremes regardless of the level of urbanization of the recording station (Easterling et al, 2000). However, for the time period 1950-1996, Gaffen and Ross (1998) noted a positive trend in extreme daytime and nighttime temperatures, primarily in urban areas indicating a correlation between rising minimum daily temperatures and increasing atmospheric greenhouse gases. The warming trend has been found to be approximately three times greater in urban areas than in rural areas, and twice as great in urban areas as in suburban areas for the years 1960-1996 (DeGaetano & Allen,

2002). Other studies show that for the period from 1951 to 1989 there has been an increasing trend in the minimum daily temperature (nighttime temperature) while there has been no corresponding increasing trend in maximum daily temperatures, meaning that nights are generally warmer now than they have been in the past, a trend exacerbated by the UHI (Easterling, 2000) (Alexander et al., 2006). In a humid climate the UHI may only have a 3˚- 4˚C differential during the day between the urban core and surrounding rural areas, while at night the differential can increase to approximately 11˚C (Jenerette et al., 2007). The trend of rising minimum daily temperatures has been found to occur on the global scale, ruling out regional bias (Alexander et al., 2006).

1.2.1.1 Land Cover and the Urban Heat Island

1.2.1.1.1 Vegetation

The urban built environment has the potential to increase the effect that an EHE has on mortality rates via the urban heat island effect, especially in the poorest neighborhoods of a city. Understanding how climate change impacts urban centers is important because the majority of heat related morbidity and mortality occurs in large cities, with the majority of those deaths happening among the city's poorest residents (Harlan, Brazel, Prashad, Stefanov, & Larsen, 2006). Microclimates exist within the urban arena creating spatial variations in temperature within the urban boundary that correspond to the socio-economic status of the population (Hope et al., 2003). Urban poverty, especially in the age 65 and up demographic, has been shown to be the most influential variable on mortality when studying the urban spatiality of EHEs (Johnson & Wilson, 2009). Proximity to the urban core has not been shown to be a significant factor for determining the spatial characteristics of mortality within the UHI, rather it is the spatial and

vegetative configuration of the neighborhood within the urban core that largely determines the extent of the UHI effect (Harlan, Brazel, Prashad, Stefanov, & Larsen, 2006). Poor city residents often lack financial and political resources necessary to mitigate the factors that lead to neighborhood scale warming, including increasing vegetative cover, reducing the density of housing, and creating vegetated open space (Harlan, Brazel, Prashad, Stefanov, & Larsen, 2006).

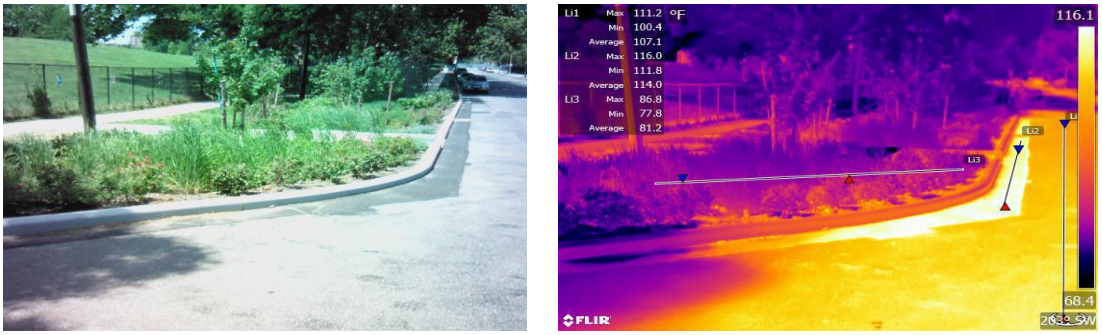

Figure 4 Vegetation has a profound effect on land surface temperature. Photo courtesy of Dr. Stuart Gaffin, Columbia University Earth Institute, Center for Climate Systems Research.

1.2.1.1.2 Soil Moisture

Antecedent soil moisture has been shown to be negatively correlated with surface temperatures at both the local and regional scale. The lower the soil moisture content on a regional scale, the higher the maximum temperature during an EHE (Durre, Wallace, & Lettenmaier, 2000) (Mueller & Seneviratne, 2012). Dry soils reduce the latent heat cooling that normally occurs at nighttime, increasing the minimum daily surface temperature and amplifying surface temperature anomalies by nearly 40% (Fischer, Seneviratne, Vidale, Lüthi, & Schär, 2007).

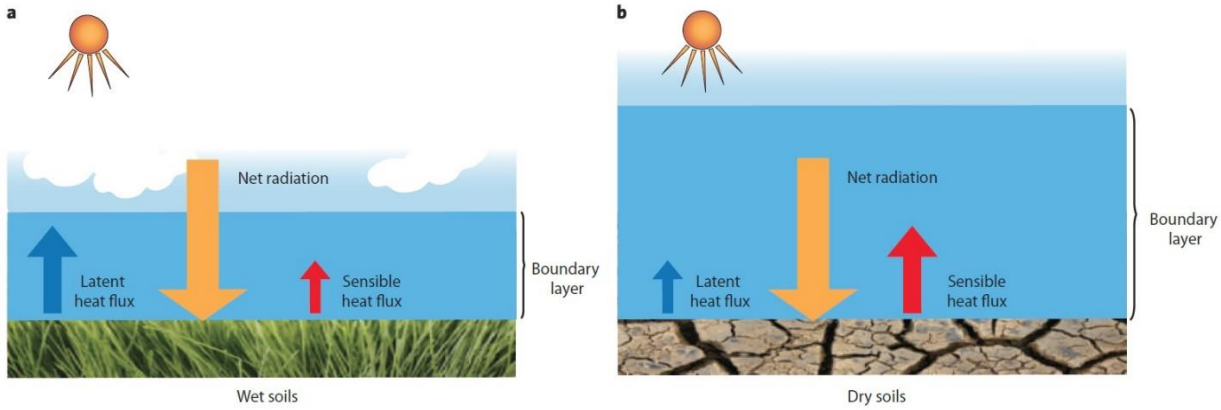

Figure 1 | Schematic of the net radiation budget at the land surface. **a**, In areas with high soil moisture, the latent heat flux by evaporation and transpiration dominates, enhancing cloud formation and a tendency for cooling. **b**, By contrast, if the soil-moisture deficit is high, the dry soils raise the sensible heat flux, producing a deeper, warmer, drier low-level atmosphere. This process inhibits convection and cloud formation and creates a positive feedback loop. Using observations for Europe, Hirschi and colleagues[3] show that the frequency and duration of hot extremes seems to scale with the strength of the antecedent drying of the land surface and that regional climate models can capture this relationship for drier climate regimes.

Figure 5 Credit Nature.com

Soil moisture does not only influence surface temperature by reducing the latent heat flux, it also influences tropospheric circulation patterns by creating a positive feedback mechanism via a surface heat low and enhanced ridging in the mid-troposphere (Vose, Karl, Easterling, Williams, & Menne, 2004). Reinforcing the findings of this study were the results of another study that found that extremely hot days are more influenced by soil moisture deficit than are days of average temperatures, largely due to atmospheric circulation changes (Mueller & Seneviratne, 2012). EHEs in Europe have been shown to be enhanced by dry soil conditions in the Mediterranean area, indicating that reduced soil moisture conditions not in proximity of urban centers can influence urban climate due to the coupling of atmosphere and soil moisture dynamics (Vautard et al., 2007). The changes in atmospheric circulation patterns caused by reduced soil moisture conditions can lead to a weakening of nighttime winds which means that cooling by advection is also reduced and thus daily minimum temperatures are increased (Grossman-Clarke, Zehnder, Loridan, & Grimmond, 2010).

for an equal number of cooling days as a moderate climate (Thevenard, 2011). Thus removing one of the largest barriers to widespread adoption of green roof technology (Clark, Adriaens, & Talbot, 2008).

1.2.2 The Influence of Green Roofs on Pollutants

The removal of ground level ozone from the atmosphere by vegetation is difficult to quantify since ozone is considered a secondary pollutant. The level of ozone present in the near surface atmosphere depends upon the presence of the precursors necessary to form ozone: volatile organic compounds, solar radiation, and NOx. The formation of ozone happens in the atmospheric boundary layer at time scales of approximately 1 hour (Anderson et al., 2001). Atmospheric conditions conducive to creating a high ozone days in Atlanta, GA occurred on days that were hot, had low humidity, and had low atmospheric mixing heights early in the day and high atmospheric mixing heights in the evening (Diem, 2009). The convective currents carry the ozone from the surface up to a stream of fast moving air that is the major mechanism for atmospheric pollutant transport and occurs at about 30m above the surface (Anderson et al., 2001). In Atlanta, Georgia, high ozone days are associated with atmospheric conditions where the metropolitan area is on the western side of an atmospheric trough that encourages the transport of ozone precursor pollutants into the Atlanta metro region from the Ohio River Valley (Diem, et al 2010).

Vegetation can act as both a source and a sink for ground level ozone; as a source of biogenic volatile organic compounds that are precursors to the formation of ozone, and as a sink via wet or dry deposition, and chemical conversion via absorption. Vegetation sinks pollutants as atmospheric gases can be absorbed by vegetation and either stored in the mass of the plant or converted to other gases via respiration; or pollutants may stick to the exterior mass of the plant

until they are either absorbed by the plant or they are washed off and adsorbed into the soil (Currie & Bass, 2008). Trees can also produce biogenic VOC's such as isoprene and monoterpenes that are the precursors to the formation of ground level ozone (Mochizuki et al., 2015). When planning a landscape project in an urban setting it is vital to select tree species that are low VOC emitters in order to reduce the amount of ozone that would form from any biogenic VOC's emitted by the installed vegetation (Churkina, Grote, Butler, & Lawrence, 2015). Trees are not the only type of vegetation contributing to the biogenic VOC inventory; expanses of lawn grasses emit significant amounts of VOC's each time they are cut (Churkina, Grote, Butler, & Lawrence, 2015) and expanses of lawn grasses are also strongly associated with land parcels that produce excess heat thereby contributing to the urban heat island (Stone & Rodgers, 2001).

A study using Detroit, MI as a study area estimated that if 20% of the city's roofs were converted into extensive green roofs, then approximately 889 tons of NO_2 could be removed from the atmosphere (Clark, Adriaens, & Talbot, 2008). Research using Chicago, IL as the study area found that of the pollutants directly removed by an extensive green roof, ozone accounted for 52%, NO_2 for 27%, PM^{10} for 14%, and SO_2 for 7% of the total pollutants removed. Peak pollutant removal occurred in May which corresponds to the peak growing season in the Chicago area (Yang, Yu, & Gong, 2008). Green roofs also reduce atmospheric pollutants indirectly by reducing the demand for air conditioning, which in turn reduces the amount of coal burned to produce the energy to operate HVAC systems leading to a reduction in primary emissions (Rosenfeld, Akbari, Romm, & Pomerantz, 1998).

1.2.3 The Influence of Green Roofs on Stormwater Management

Stormwater runoff poses a threat to municipal water supplies and has the potential to contaminate urban waterways. Rain that would have been absorbed or evapotranspirated by

plants on naturally vegetated land, runs off of the impervious surfaces of the urban built environment and enters the municipal waste water treatment system instead (Morgan, Celik, & Retzlaff, 2013). Calling it one of the top reasons that water quality standards are not being met in urban areas, the U.S. Environmental Protection Agency has deemed stormwater runoff as the biggest threat to water quality nationwide (Garrison & Horowitz, 2012).

One of the primary benefits of a green roof is their ability to reduce and slow the stormwater runoff from precipitation events, preventing municipal sewer systems from becoming overwhelmed and overflowing. According to the EPA SWMM model, conventional roof consisting of impervious surface has a stormwater run-off rate of 88%. Naturally vegetated land has an annual stormwater run-off rate of about 40%, generally occurring during either intense precipitation events or events that occur when the soil is still saturated from a previous storm. How close a green roof comes to approximating the natural environment in terms of run-off depends on the depth of the growing medium and the type of vegetation on the roof (Nardini, Andri, & Crasso, 2012). During small precipitation events a green roof has been shown to be very effective at reducing peak runoff and increasing lag time and duration of response time (Polinsky, 2009). An extensive green roof has been estimated to have the ability to capture 35% to 100% of precipitation, depending on the growth medium and the size of the precipitation event (Zhang et al., 2015).

Green roofs also act as a filter for stormwater by removing many of the pollutants that are present before they reach the watershed. The concentration of Total Suspended Solids (TSS) can be reduced, and pH can be increased when stormwater is filtered through a green roof (Zhang et al., 2015) (Morgan, Celik, & Retzlaff, 2013). The overall pollutant load added to the watershed is decreased because the amount of runoff is been decreased. However, certain pollutants have

been shown to increase in runoff from a green roof, particularly phosphorous and potassium with the amounts of these pollutants decreasing as the roof ages (Garrison & Horowitz, 2012).

1.3 Research Question and Objectives

Climate plays a large role in the energy performance of a green roof since their performance is closely linked to the ability of plants to evapotranspirate and intercept solar radiation. What is not well known are the potential effects of green roofs in warmer and wetter urban areas in the United States; therefore, this research focuses on Atlanta, the largest city in the southeastern United States. Peer reviewed studies on green roof technology specific to the Atlanta study area have not been done, creating an opportunity for research as shown in figure 6.

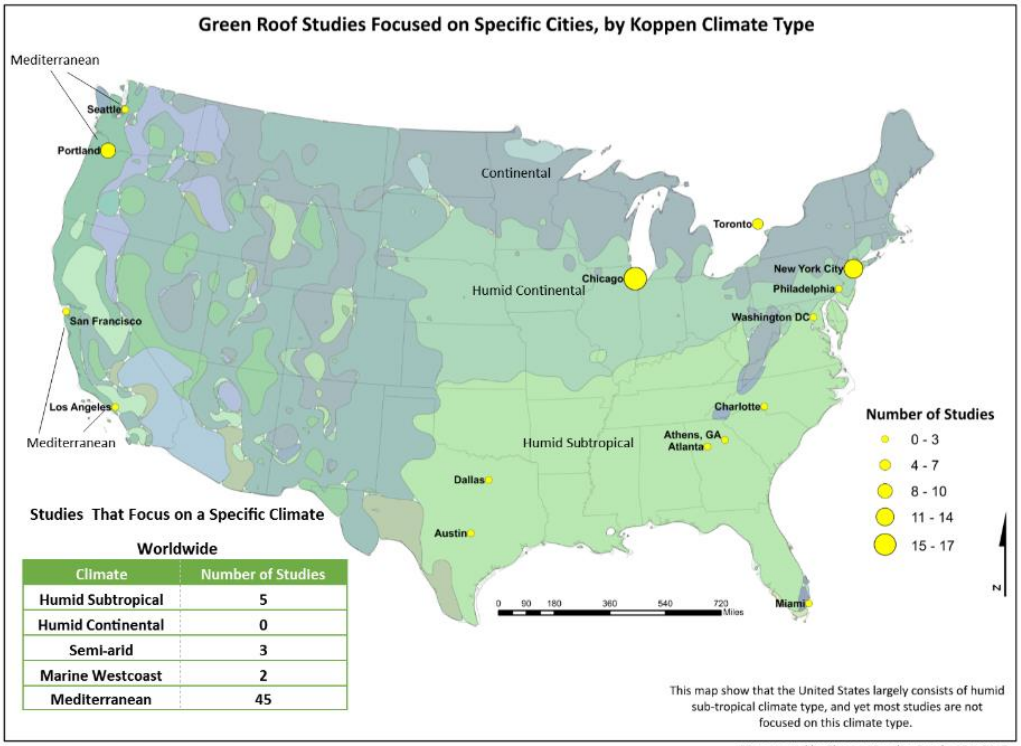

Figure 6 Green roof Study Locations

How closely the addition of green roofs can mimic the natural environment in terms of stormwater runoff abatement, pollution removal, and temperature reduction in a city located in a sub-tropical climate is rarely studied. The research focus is as follows: How and to what extent would green roofs improve environmental conditions in a humid subtropical city? The objectives derived from this question are (1) determine the spatiality of the Atlanta urban heat island, (2) determine the extent of stormwater runoff generated by impervious surfaces in Atlanta, and (3) determine the potential of a green roof to help reduce atmospheric pollutants NO_2, SO_2, 0_3, and PM_{10}.

2 The Study Area

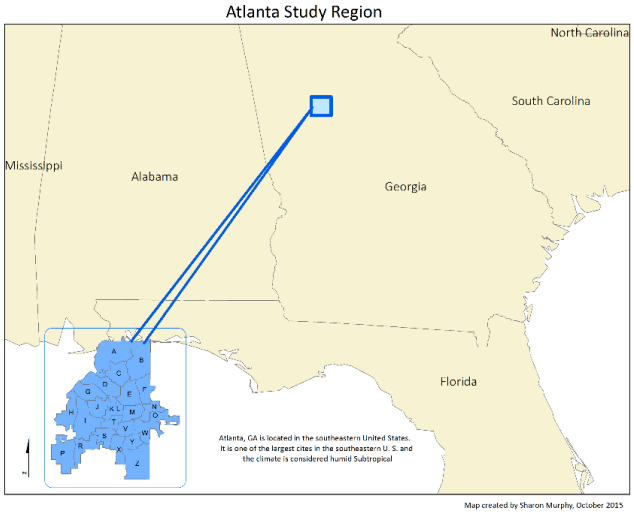

Figure 7 Atlanta, GA

2.1 Atlanta

As one of the fastest growing metropolitan areas in the United States, the urban form of Atlanta has grown unencumbered by the physical boundaries that often limit the spatial extent of major metropolitan cities (Figure 7). By modeling Atlanta's growth patterns, Yang and Lo (2002) have predicted that almost all of Atlanta's greenspace could disappear if current growth patterns persist and state that specific actions would need to be taken to encourage the preservation of greenspace. Already, the sprawling nature of the Atlanta Metropolitan Statistical Area (MSA) has led to an increase in ambient temperature in the urban core due to the advection of air heated in the suburban/urban interface (Stone & Rodgers, 2001). The sprawling nature of the Atlanta MSA has also led to a multinucleated structure where nodes of downtown-like development exist (Fujii & Hartshorn, 1995) and this leads to a spatially heterogeneous UHI (Buyantuyev & Wu, 2010).

Atlanta is classified as a humid subtropical climate using the Koppen Climate System. This climate is characterized by hot and humid summers and mild to cool winters, and plentiful precipitation year round (Diem, 2013). Figure 8 shows the annual temperature and precipitation distribution of Atlanta.

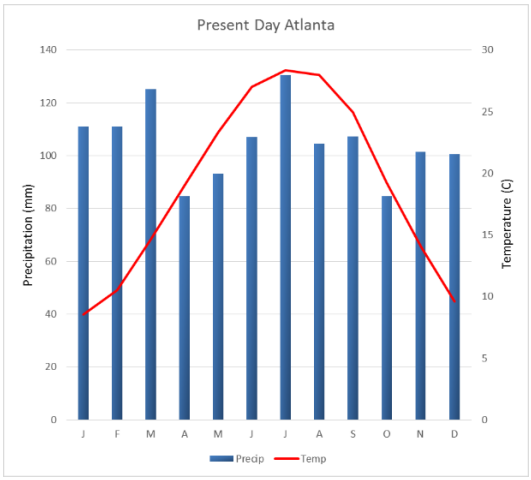

Figure 8 Atlanta Climograph

2.2 Georgia State University

The ability to stymie the impacts of urbanization on the environment are often deployed in a patchwork style because urban properties are generally owned and controlled by disparate corporate entities with no ties that bind them together. Universities located in an urban setting are ideally suited to help mitigate the urban heat island phenomenon due and their large campus footprint under the control of a single owner, which allows for a cohesive plan of action over a large area. Located in the heart of Atlanta, Georgia State University has developed a campus landscape master plan that will add greenspace to a campus dominated by impervious surfaces such as concrete and asphalt. Largely ignored in the master plan is the expanse of real estate that exists on the rooftops of the campus buildings. A thorough understanding of the potential impact of installing green roofs on the Georgia State University (GSU) campus may increase the likelihood that the university will adopt green roofs as part of their master plan for the campus.

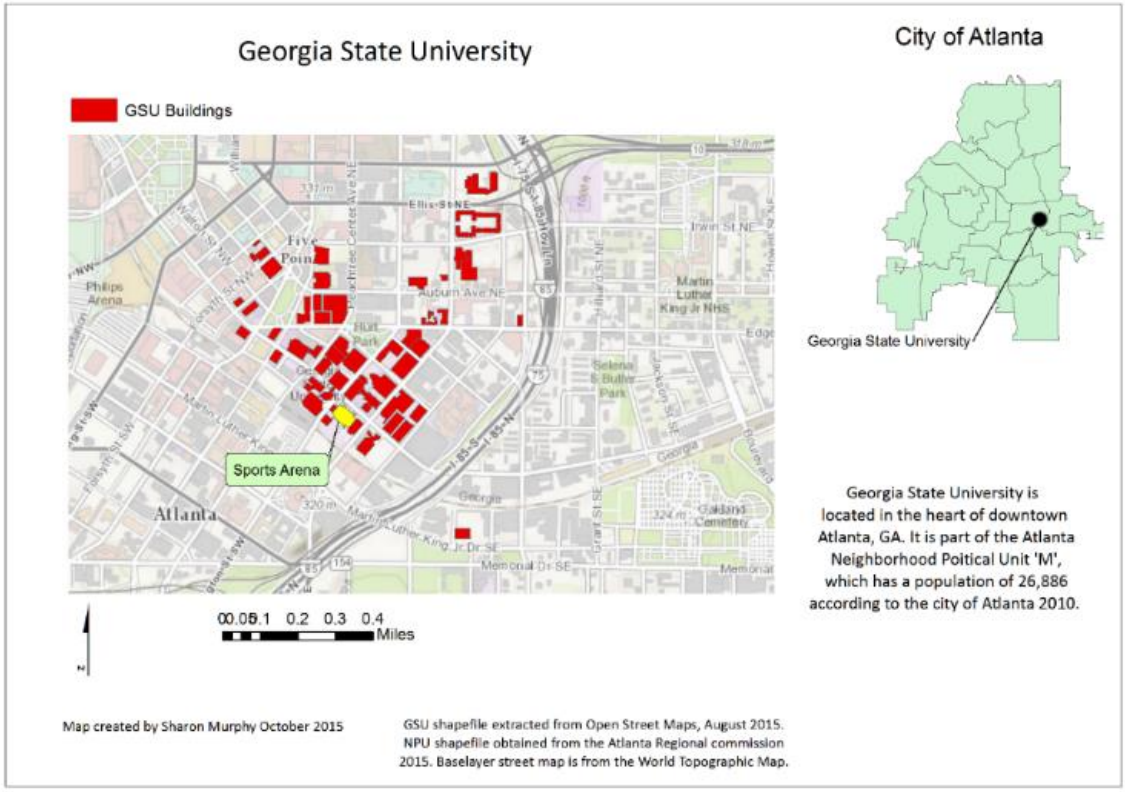

Figure 9 Georgia State University

Georgia State University is considered an open, urban campus meaning that the streets and sidewalks that transect the campus are public thoroughfares owned and maintained by the city of Atlanta (Figure 9). Located in the southeastern region of the United States, the climate of Atlanta is categorized as humid sub-tropical (Diem, Hursey, Morris, Murray, & Rodriguez, 2010). Given the unique structure and situation of each urban environment, and given that the structure and environment play large roles in the effectiveness of green roofs to mitigate the urban heat island, the results from a study performed on one city may not be replicated when the study area is changed. Climate conditions unique to Atlanta effect the number of heating and

cooling days buildings require, and also affects the vegetative growing season that in turn determines the effectiveness of green roof technology.

The campus of Georgia State University was chosen because of its location in downtown Atlanta, an area that largely consists of impermeable surfaces and little green space. Another factor in the choice of using GSU as the study region is the commitment that the GSU administration has made to increasing green space on campus. Georgia State University has developed a campus Master Plan that will create more green space at the street level, but ignores the vast expanse of exposed surface on campus rooftops. Satellite imagery shows that the rooftops of GSU buildings are largely composed of dark materials that absorb solar radiation during the day and become very hot, then slowly release this heat at night diminishing the diurnal temperature differential that leads to the UHI effect and increases EHE related mortality (Davis, Knappenberger, Michaels, & Novicoff, 2003). Importantly, the GSU Facilities Administration has expressed a desire to learn more about the benefits of green roofs at GSU with the intention of possibly installing one or more green roofs on campus. The information gained through this study has the potential to lead to an outcome that may have real world impacts.

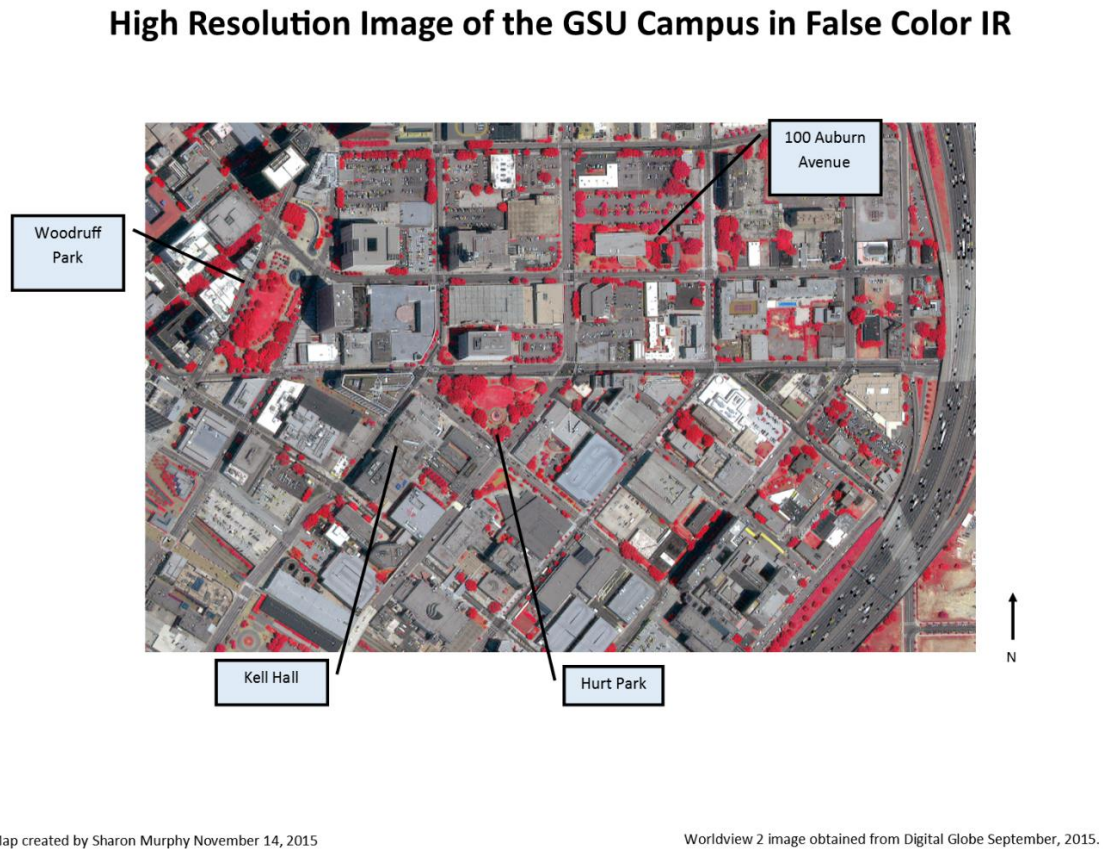

Figure 10 False color IR image of the GSU Campus

The GSU campus in high resolution, false color IR image in figure 10 shows the lack of vegetation and the large amount of impervious surface that exists on the GSU campus.

3 Methods

Determining the spatiality of the Atlanta urban heat island allowed for deeper analysis of the possible factors driving the formation of the UHI. Impervious surface rasters and NDVI rasters were created and correlated to the land surface temperature rasters. Stormwater runoff analysis combined with the impervious surface analysis created a complete picture of the current

runoff situation and based on this future scenarios were created to model climate change impacts. Landsat 5 images have a thermal band that can be converted to LST at the 120m scale, which is a much finer resolution than temperature readings reported from area weather stations can provide. This information can be combined with land classification and NDVI analysis to form a comprehensive picture of what is happening in the Atlanta metro area with regards to fine resolution temperature mapping. The potential for low impact development (LID) practices to mitigate stormwater runoff can be estimated after first determining current runoff amounts and then modeling possible LID scenarios. Data about the amount of surface area in Atlanta covered by roofs was used to determine the total contribution that roofs make to LST and the effect that various mitigation scenarios might have on the UHI. Building footprint data were obtained from Open Street Map via Metro Extracts (http://metro.teczno.com/).

3.1 Land Surface Temperature

Days representative of a typical summer day were determined based on the National Weather Service Heat Index (HI). Hourly temperature data for Hartsfield Jackson International Airport, Peachtree Dekalb Airport, and Atlanta Fulton County Airport were downloaded from the National Weather Service for the years 1999 – 2014. The heat index (T) for each day during the months of June, July, and August (JJA) for this study period were calculated, as well as the 85^{th}, 90^{th}, 93^{rd}, and 95^{th} percentiles for each day in order to prevent bias from having too many EHE, or unusually cool days. Daily maximum temperatures ($T_{max)}$ were then analyzed to determine where they fell in relation to the average temperature for that day during the study period to determine what days could be categorized as an extreme heat event (EHE).

Once ‘typical’ days were identified, satellite images were reviewed in order to find an image that was taken on a ‘typical’ day, and was also cloud free. Level one satellite imagery was obtained from the U.S. Geological Survey database (Earthexplorers.usgs.gov). To establish a baseline for our results and make sure that this day represented a typical spatial distribution of temperature in Atlanta, all the cloud free images for JJA during the study period were analyzed in an identical manner to the EHE. Due to differences in water vapor content in the atmosphere which can alter at-sensor brightness values, it is not appropriate to compare the derived LST between different time periods. Instead, the spatiality of the temperature distribution across the image acquisition dates should be the primary focus of the comparative analysis (Chen, Zhao, Li, & Yin, 2006). To account for this, a composite from the processed images was derived and used as a representation of a typical summer day in Atlanta.

The Landsat 5 TM images that were chosen were converted to visual representations of land surface temperatures using the method developed by Sobrino et al. (Sobrino, Jiménez-Muñoz, & Paolini, 2004). Using remote sensing image processing software, the images were subset so that only the Atlanta region was subjected to image processing and analysis. Atmospheric correction was applied to each image to counteract the distortion that wind speed, specific humidity, and air temperature have on path of solar radiation and thus on the final computation of LST (Dousset & Gourmelon, 2003). A Normalized Difference Vegetative Index (NDVI) raster was produced from each image using Landsat band three (red) and four (near infrared) as shown in Equation 1:

Equation 1 NDVI

$$\frac{nir - r}{nir + r}$$

Landsat 5 produces 8 bit images composed of pixels with digital number (DN) values assigned to them ranging from 0 – 255 and corresponding to the surface reflectance assigned to that pixel. DN's need to be converted to radiance values for the derivation of LST via equation 2 (Barsi, Hook, Schott, Raqueno, & Markham, 2007):

Equation 2 Radiance

$$R = .055376 * Tb + 1.18243$$

Where R = radiance

.055376 = Landsat 5 gain value for band 6

Tb = DN thermal band (band 6)

1.18243 = Landsat 5 bias value for band 6

These radiance rasters were then converted to temperature rasters, expressed in degrees Kelvin using equation 3 (Yale, 2010):

Equation 3 Radiance to temperature in Kelvin

$$\frac{1260.56}{\left(Ln\left(\frac{607.76}{B_r}\right)+1\right)}$$

Where:

1260.56 is a band specific thermal conversion constant in kelvin

607.76 is a band specific thermal conversion constant in $w^{-2*ster*\mu m}$

B_r is the radiance band created in the previous step.

The resulting temperature raster contains values that reflect the at-sensor brightness temperature in degrees Kelvin. Further processing is required to complete the conversion to land surface temperature.

An emissivity raster was developed for each image from the NDVI rasters created in equation 1, using equation 4 (Sobrino, Jiménez-Muñoz, & Paolini, 2004).However, there are several assumptions associated with the execution of this formula:

1. NDVI values less than 0.2 are considered bare soil and an emissivity value of .972 is assumed.
2. NDVI values greater than 0.5 are considered healthy vegetation and an emissivity value of .99 is assumed.
3. NDVI between .2 and .5 are considered mixed pixels and so equation 4 must be used to calculate the emissivity values of these pixels. Steps to completing this equation in can be found in Appendix A.

Equation 4 Emissivity

$$\mathcal{E}_{Tb} = .004 * Pv + .986$$

Where $\mathcal{E}_{Tb}$ is the emissivity of thermal band 6.

.004 is the standard deviation of the emissivities of 49 soil spectra.

.986 is the average emissivity of the soil rasters and the vegetated rasters.

Pv is the percentage of vegetation present in a pixel and is calculated using equation 5:

Equation 5 Percentage Vegetation

$$Pv = \left(\frac{NDVI - NDVImin}{NDVImax - NDVImin}\right)^2$$

Where P*v* is the percentage of vegetation per pixel with NDVI between 0.2 – 0.5.

NDVI*min* is 0.2

NDVI*max* is 0.5

The next step in converting the satellite images to LST maps is to use the raster created in equation 15 as part of equation 16 (Weng, Lu, & Schubring, 2004):

Equation 6 Land Surface Temperature in Kelvin

$$LST = \frac{Tb}{\left(1 + \frac{(Wp * Tb)}{C} \ln[\![\varepsilon)]\!]\right.}$$

Where LST is the land surface temperature expressed in degrees Kelvin.

Tb is the thermal band raster.

Wp is the peak wavelength of the emitted radiance.

Equation 7 Land Surface Temperature

$$C = h*c / s\ (1.438 * 10^{-2}\ m\ K)$$

Where h is Planck's Constant ($6.626 * 10^{-34}$ Js).

s is the Boltzman Constant ($1.38 * 10^{-23}$ J/K).

c is the speed of light ($2.998 * 10^{-8}$ m/s).

The new raster produced as the result of equation 6 represents the LST in degrees Kelvin so it needs to be converted into degrees Celcius using the equation 8:

Equation 8 Convert Kelvin to Celcius

$$Tc = LST - 273.15$$

Where Tc is temperature expressed in degrees Celsius.

3.2 Spatial Investigations of Land Surface Temperature

Giving context to the LST maps was essential for understanding the meaning behind their spatial temperature distributions. A shapefile of the Atlanta Neighborhood Political Units (NPU) was obtained from the Atlanta Regional Commission GIS database. Atlanta consists of

25 NPU's that are operated by citizens to create a liaison between city government and the citizenry. The Atlanta NPU's were extracted from the LST raster so that statistics would not include pixels outside of the city of Atlanta boundary. The raster produced from this process was used to run zonal statistics in order to get descriptive temperature statistics per NPU, including the T_{min}, T_{max}, and T_{avg}.

The mean of the pixels with the top 5% of land surface temperatures and the mean of the pixels with the bottom 5% of land surface temperatures were examined to find out the range of LST in Atlanta. The means of the top and bottom 5% were also analyzed for their numerical difference in order to see if there was consistency between the image days in terms of peak values and low values. Extreme hot and cold values were identified for each day. To determine the environmental impact that green roofs may have at the city and campus scale, land surface temperatures for 6 cloud free summer days were created. Pearsons R was also used to check for spatial correlation of heat between the image days in order to determine if there was a consistent spatial distribution of heat in the city of Atlanta.

Further visualization of the spatiality of the urban heat island in Atlanta was necessary to see the extent and magnitude of the temperature gradient. The raster derived from the means of each of the typical, cloud free, summer days was used to visualize the Atlanta urban heat island. Using the GSU campus as the centroid, three two mile wide, circular buffers were created in order to see if a temperature gradient exists from the GSU campus outward. In total this created four zones, including the GSU campus, where the mean temperature for each zone was derived using zonal statistics.

3.2.1 Analysis of the Relationships between Land Cover and Land Surface Temperature

The extent of vegetative land cover varies widely across the Atlanta metro region. Analyzing land cover was necessary to see if a relationship exists, and how strong that relationship might be, between land cover and LST at the NPU level. Impervious surface data was downloaded from the National Land Cover Database (2011) and clipped to match the Atlanta shapefile extent. The NLCD dataset is raster data at 30m resolution based on Landsat data from 2011. This data, which was downscaled to 30m in its original form, was scaled up to 120m extent in order to match the resolution of the Landsat TM thermal band resolution and prevent the introduction of an ecological fallacy. The percent of impervious surface per NPU was calculated and then tested for significant correlation with mean NPU temperatures using Pearson's product-moment correlation tests (one-tailed; $\alpha = 0.01$) with t.

The LST, NDVI, and Impervious Surface rasters were converted to point data that was analyzed to see if a correlation existed between LST and NDVI, and LST and Impervious Surface using Pearson's product-moment correlation tests (one-tailed; $\alpha = 0.01$) with t. Pearsons R was also used to check for spatial correlation of heat between the image days in order to determine if there was a consistent spatial distribution of heat in the city of Atlanta.

An Atlanta-specific dataset was created using a high-resolution satellite imagery. Worldview 2 satellite imagery has a panchromatic spatial resolution of 0.5m and a multi-spectral resolution of 1.86m, providing highly detailed land cover data. The impervious surface analysis was performed using an unsupervised classification with 30 initial classes and 20 iterations, with the 30 initial classes being reclassified into two classes: impervious and pervious.

Scatterplots were created and tested for significant correlations between LST and impervious surface for each image day using Pearson's product-moment correlation tests (one-tailed; $\alpha = 0.01$) with t. The percent of impervious surface per NPU was calculated and then correlated using Pearson's R with the mean temperature raster developed from Landsat data for this study.

Scatterplots were also created for the Normalized Difference Vegetative Index (NDVI), a measure of the health, or 'greenness' of vegetation. The NDVI is expressed as a ratio with healthier vegetation having a higher value. The NDVI scatterplots were also tested for significant correlations with LST for each image day.

High resolution Worldview 2 imagery of the city of Atlanta was analyzed for impervious surface and NDVI at the .5 meter scale. The Worldview 2 satellite is owned by Digital Globe, who requires that each image have at least a 2 kilometer width in every direction of the area of interest. This necessitated adding a buffer to the exterior of the image in order to widen the narrowest parts of the city of Atlanta boundaries to acceptable standards for the NDVI analysis.

3.2.2 Extraction of Atlanta Roofs and Examination of Roof Surface Temperatures

To understand the impact that green roofs have on the city of Atlanta it was necessary to extract roof data of Atlanta, and of GSU. Data about the amount of surface area in Atlanta covered by roofs was used to determine the total contribution that roofs make to stormwater runoff and the effect that various mitigation scenarios might have. Building footprint data were obtained from Open Street Map via Metro Extracts (http://metro.teczno.com/). 30m temperature values were examined only for roofs equal to or larger than 14,400m^2 since this is equivalent to a single Landsat TM thermal band pixel, the finest resolution available for this study. Histograms of the roof temperatures were created to determine the temperature range of relatively hot and

relatively cool roofs. The contribution that roofs have to total LST, and to LST under various green roof scenarios was estimated using equation

3.3 Estimation of Pollutant Removal

There are no studies that quantify the amount of pollutants removed from the atmosphere by green roofs in a humid subtropical climate. The values for this study are based on a study focused on Chicago, IL (Humid Continental climate type) and assumed that a roof consists of short grasses. Total annual pollutant removal rates were calculated for the city of Atlanta and the GSU campus for scenarios assuming 10%, 20%, 50%, and 100% of roofs being vegetated. Pollutants examined included NO_2, SO_2, PM_{10}, and O_3 using coefficients from Yang et al (2008) for short grasses, multiplied by the percentage of roof area covered by vegetation. Differences in pollution removal between species was examined using values from a study by Speak et al (2012) that compared a cultivar of the popular green roof plant Sedum album, to three species of grasses in a study based in a Marine West Coast climate type. Removal rates per species were calculated at the city of Atlanta scale and the GSU campus scale using different green roof percentage scenarios of 10%, 20%, 50%, and 100%. Results were derived using the potential roof area vegetated multiplied by the coefficient from the study.

3.4 Estimation of Mean Surface Temperature and Cumulative Stormwater Runoff under Multiple Scenarios

Mitigating stormwater runoff is one of the primary reasons cited for the installation of a green roof. The green roof partially mimics the land that existed before the land was built on, but the degree to which a green roof performs in that capacity depends upon the depth of the growing medium and the type of vegetation present on the roof. Most precipitation that falls on metro Atlanta annually, falls in the form of rain. While it does snow in Atlanta, precipitation is

not held in this state for more than a few days and it quickly becomes available to vegetation as it melts. This means that monthly precipitation totals represent precipitation immediately available for evapotranspiration and is not held in crystalized form until Spring.

Four green roof scenarios were used to estimate the impact that vegetative roofs might have on Atlanta LST: City extents of present day coverage, 10%, 20%, 50%, and 100% of vegetated roofs. The hypothetical temperatures were derived based on a formula that weighted the percentage of impervious surface, roof area, and percent of green roof coverage as shown in equation 9. This analysis was repeated at the GSU campus scale in order to see if scale made any difference in LST scenarios.

Equation 9 Estimating LST for Various Green Roof Scenarios

$$(\%green\ roof * estimated\ green\ roof\ temperature) + (\%\ of\ remaining\ Atlanta\ roofs * Mean\ of\ Atlanta\ roof\ temps) + (\%\ of\ remaining\ Atlanta\ surface\ area * Mean\ Atlanta\ temp\ for\ that\ day)$$

Where the estimated temperature of a green roof at 11a.m. was determined by subtracting 18°C from the mean temperature of the roofs (Dvorak & Volder, 2013)

Similar scenarios were used to analyze stormwater runoff at the GSU campus and the Atlanta scale with the additional variable of growing medium depth. Green roofs are cultivated in a special growing medium that ideally should consist of 20% organic matter to 80% inorganic matter according to FLL guidelines. The EPA Stormwater Management Model (SWMM) was used assuming the following parameters: a drain rate of standing water of .04 inches per hour, land cover of 41% forest, 19% lawns, and 40% impervious surface. Precipitation and evaporation data for the past 30 years was retrieved from Atlanta Hartsfield Jackson International Airport.

3.4.1 Stormwater Runoff

An estimate of the annual amount of stormwater runoff was necessary in order to form a complete picture of the effects that green roofs may have on the environment. The total amount of impervious surface as calculated from the Worldview 2 satellite image was used to estimate the total annual stormwater runoff from impervious surfaces in Atlanta. The EPA National Stormwater Calculator was used to determine what the total annual stormwater runoff would be with varying degrees of re-vegetated areas to see what impact native vegetation has on the amount of annual runoff.

The amount of annual stormwater runoff that the roofs of Atlanta and the GSU campus contribute was calculated to see what the conventional roofs contributions are to stormwater runoff at different scales. The EPA National Stormwater calculator was again enlisted to help formulate the impact that green roofs of varying depth would have on the runoff. Future runoff amounts were also estimated based on climate models that predict the southeastern region of the U.S. becoming warmer and wetter as the climate changes. The results from the EPA SWMM were converted into gallons and totals were calculated for Atlanta and GSU.

The EPA National Stormwater Calculator is based on the EPA Stormwater Management Model (SWMM) which takes into account different soil types, topography, and hydraulic conductivity. This analysis used 30 years of weather data from Hartsfield Jackson International Airport, and assumes a drain rate of .4 inches per hour, and a land cover composition of 41% forest, 19% lawns, and 40% impervious surfaces for the city of Atlanta. While these assumptions do not perfectly reflect the conditions found throughout metro Atlanta, they are a good approximation that allows for a comparative analysis between different green roof scenarios involving varying depths of growing medium.

3.4.2 Precipitation

In order to construct a current climograph for Atlanta, daily precipitation data was acquired from the National Oceanic and Atmospheric Administration (NOAA) from 1985 – 2014. The mean temperature and the mean precipitation was derived from this data set for each month of the year. An analysis of the annual soil moisture budget was also based on this data set to determine what months have a surplus of soil moisture and what months have a deficit of soil moisture. This information will help to determine evapotranspiration rates and green roof performance.

4 RESULTS

4.1 Roofs in Atlanta

The impervious surface analysis reveals that Atlanta consists of 40% impervious surface, with 25% of that impervious surface being roofs. This means that in Atlanta, roofs comprise 10% of total surface area.

4.2 Land Surface Temperature and the Urban Heat Island

The results of the conversion of the Landsat 5 images to a map of land surface temperature (Figure 11) reveal a consistent spatial pattern of heat distribution within metro Atlanta between the individual image dates and the mean image dates. This finding was confirmed by the results of the temperature correlation analysis between the rasters of the image days and the raster of the mean of the image days that revealed a consistent spatial relationship with Pearsons R ranging from a low of .897 to a high of .966.

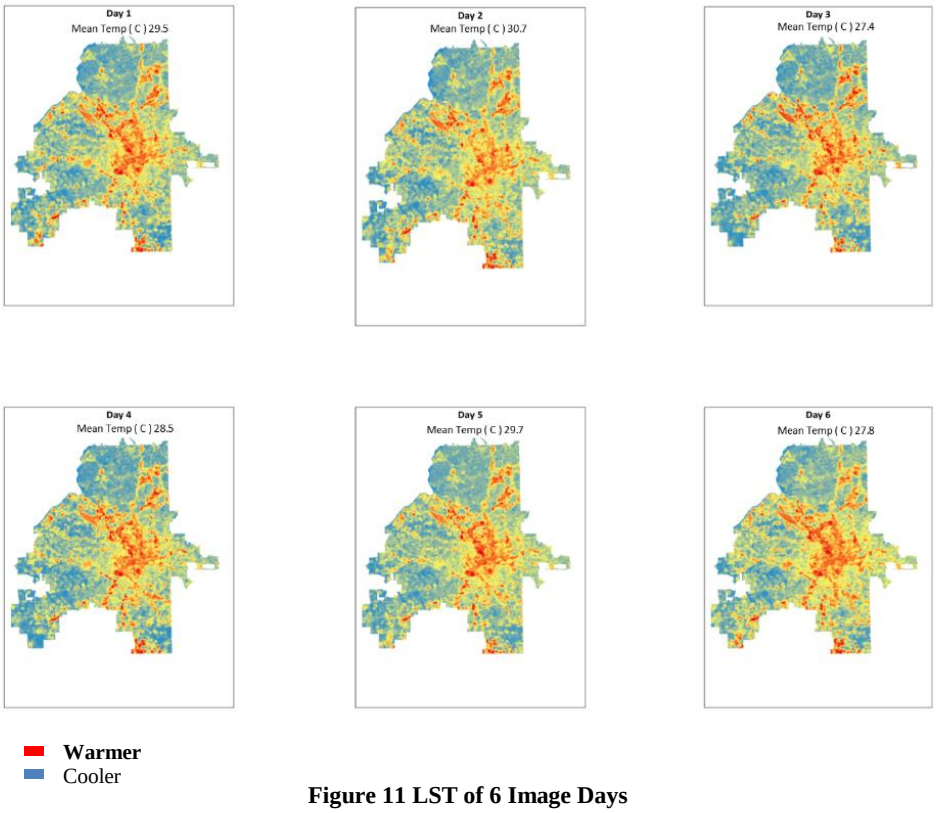

Figure 11 LST of 6 Image Days

The weather data from 1999 to 2014 revealed that 74 days fell above the 95th percentile or above on the Heat Index scale. One day was identified as meeting all criteria for the defined Heat Event Day, and also had a cloud free Landsat satellite image available. This day was categorized as Dry Tropical on the Spatial Synoptic Classification System (SSC) and fell in the 95th percentile of the mean for that day. A second image was classified on the SSC as Dry Tropical Plus and fell in the 90th percentile of the mean for that day. Another five cloud free images were classified as 'Typical' days and four of the five were classified as Dry Moderate and one as Transitional in the SSC.

Based on the raster of the mean LST of the six image days, the mean temperature for the roofs of Atlanta on the image days ranged from 33.9°C to 35.9°C, in contrast to the mean LST of the entire city of Atlanta of 27.5°C to 30.7°C. When roof temperatures were subtracted from the

data, the mean LST temperature of Atlanta on the image days was reduced to 26.7°C to 30.1°C, indicating that roofs directly contribute to the urban heat island effect. The mean temperature reduction in the Atlanta area without roofs from the Atlanta with roofs scenario ranges from .6° - .8°(C).

Table 1 Effect of Roofs on Temperature in Atlanta

Entire City	Day1	Day2	Day3	Day4	Day5	Day6
Temp in C	29.5	27.5	30.7	28.6	29.7	27.9
Mean Roof	**Day1**	**Day2**	**Day3**	**Day4**	**Day5**	**Day6**
Temp in C	36.8	33.9	35.9	35.1	36.6	34.7
City, No Roof	**Day1**	**Day2**	**Day3**	**Day4**	**Day5**	**Day6**
Temp in C	28.7	26.7	30.1	27.8	28.9	27.1

The warmest parts of the city tend to follow the major roadways and commercial development nodes. In terms of temperature, two outlier points were found: one is a very large scale server farm northwest of the urban core, and the other is a glass factory located south of the urban core. Closer to the urban core, the World Congress Center / Philips Arena complex was another hot spot, though not to the extent of the server farm or the glass factory while the Georgia Dome had the coolest roof.

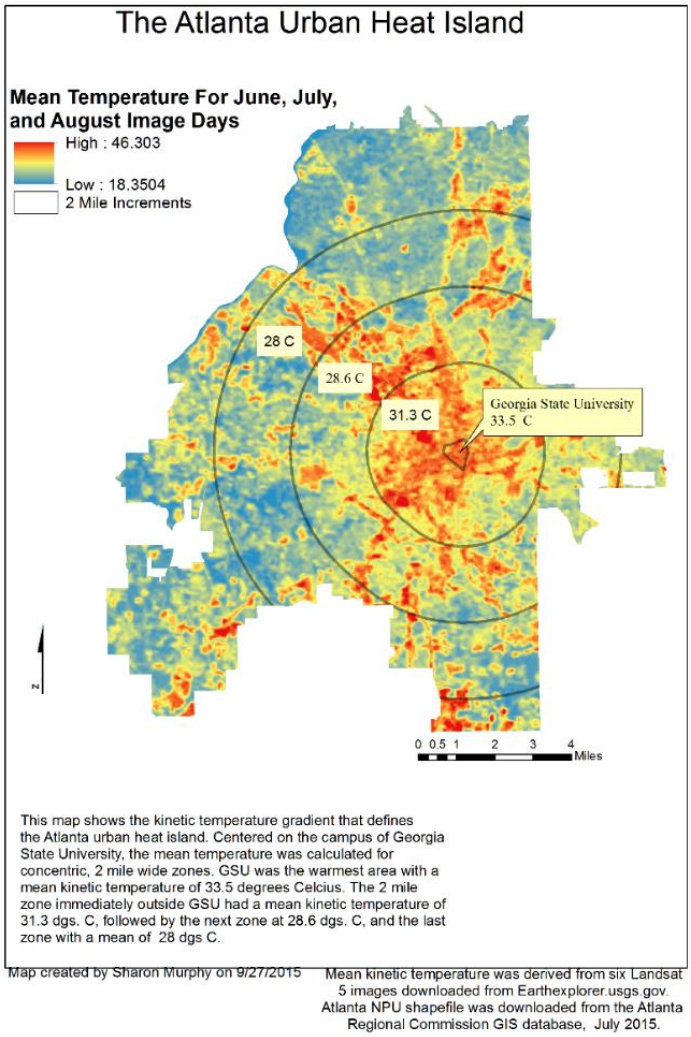

Figure 12 Map of the Atlanta Urban Heat Island Gradient

The urban core of Atlanta is the warmest area of the city with a mean temperature of 33°C, and a temperature gradient that decreases with distance from the urban core (Figure 12).

The difference between the mean temperature of the top 5% and the mean temperature of the bottom 5% reveal that the image days are fairly spatially consistent with their peak

temperature and their low temperature ranges as shown in Table 2. Examining the pixels identified as the hottest and coolest on each image revealed that the warmest pixels are the darkest rooftops while the coolest pixels are the roofs lightest in color or with the densest vegetation.

Table 2 Top 5% and Bottom 5% of Mean Pixel Values

	Mean Temp of the Top 5% In C	Mean Temp of the Bottom 5% in C	Difference
Day 1	37.2	24.8	12.4
Day 2	34.7	23.4	11.3
Day 3	36.8	26.9	9.9
Day 4	35.8	24.2	11.6
Day 5	36.9	25.7	11.2
Day 6	35.2	23.1	12.1

The histogram analysis of roofs with areas greater than 14,400m^2 show the distribution is normal and fairly consistent in terms of the mean and the range of values (Figure 13).

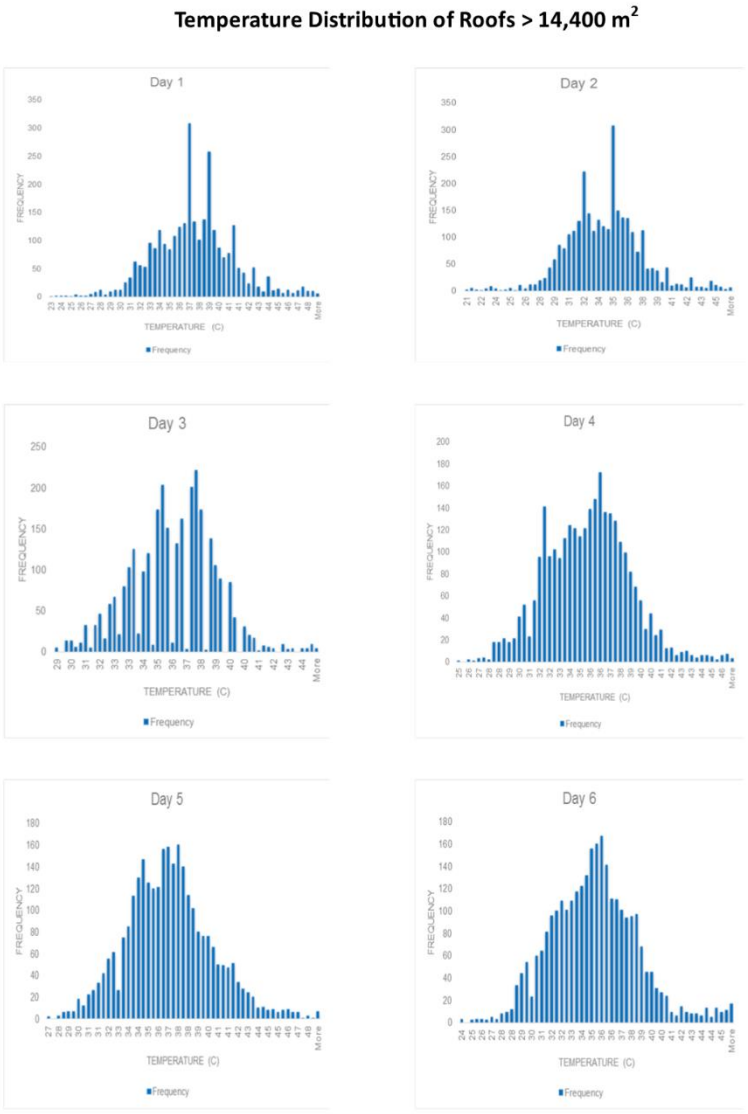

Figure 13 Histograms of Image Days

At the scale of the NPU, it is no surprise to find that the NPU's with the highest amount of impervious surfaces also have the highest mean LST. GSU is part of NPU M and this NPU has the highest percentage of impervious surface of all the Atlanta NPU's at 76% (Figure 14).

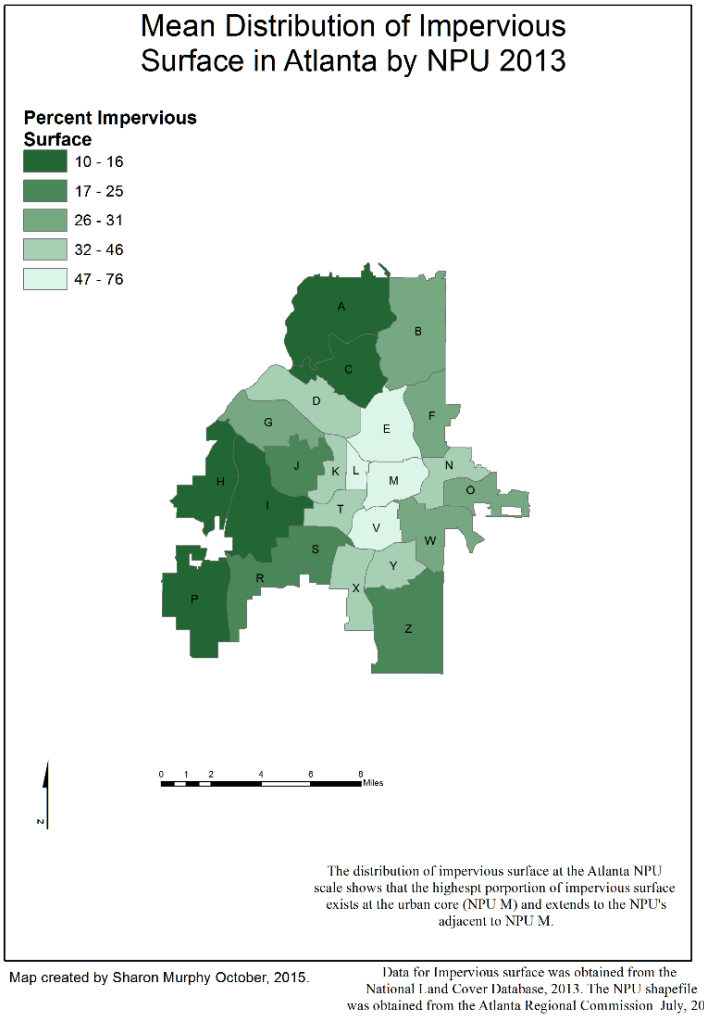

Figure 14 Impervious Surface by Atlanta NPU

NPU M is also the warmest NPU with a mean temperature of 33.5°C. The mean correlation coefficient of impervious surface and land surface temperature in Atlanta is a strong .80. There was no significant correlation between race and temperature or population and temperature.

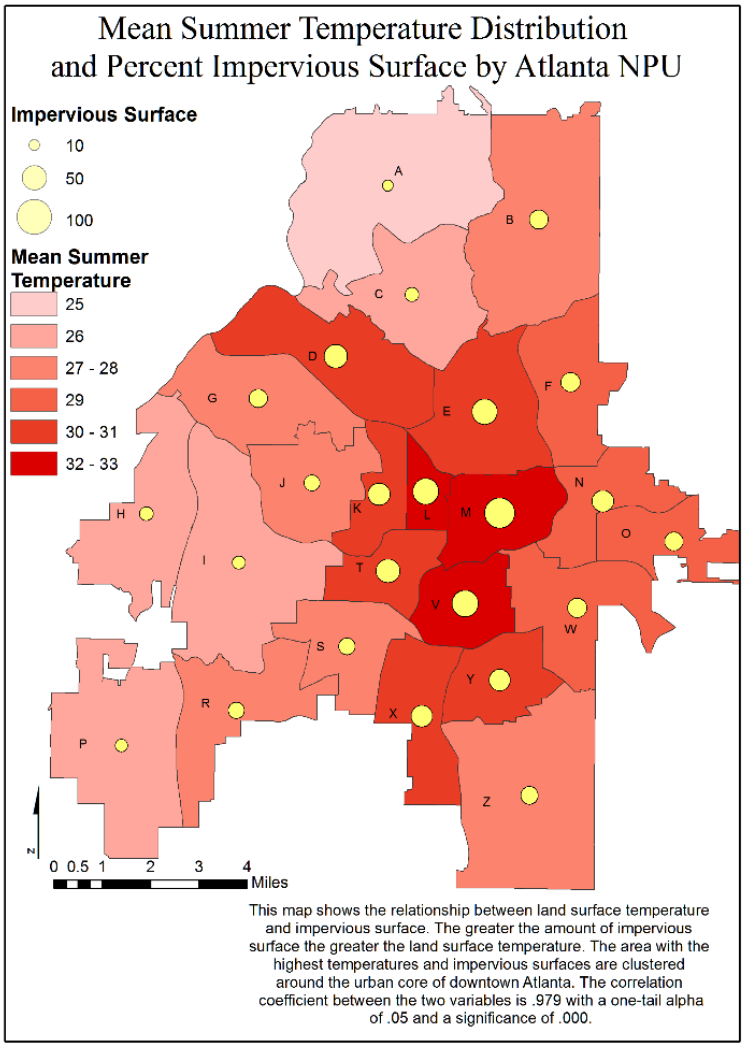

Figure 15 Map of the distribution of impervious surfaces in Atlanta by NPU

4.3 Relationship between land surface temperature and vegetative cover

Scatterplots as shown reveal a strong negative correlation between NDVI and temperature (Figure 16). The correlations range from -.79 to -.84, indicating that as NDVI increases, LST decreases with a significance of 0.0000.

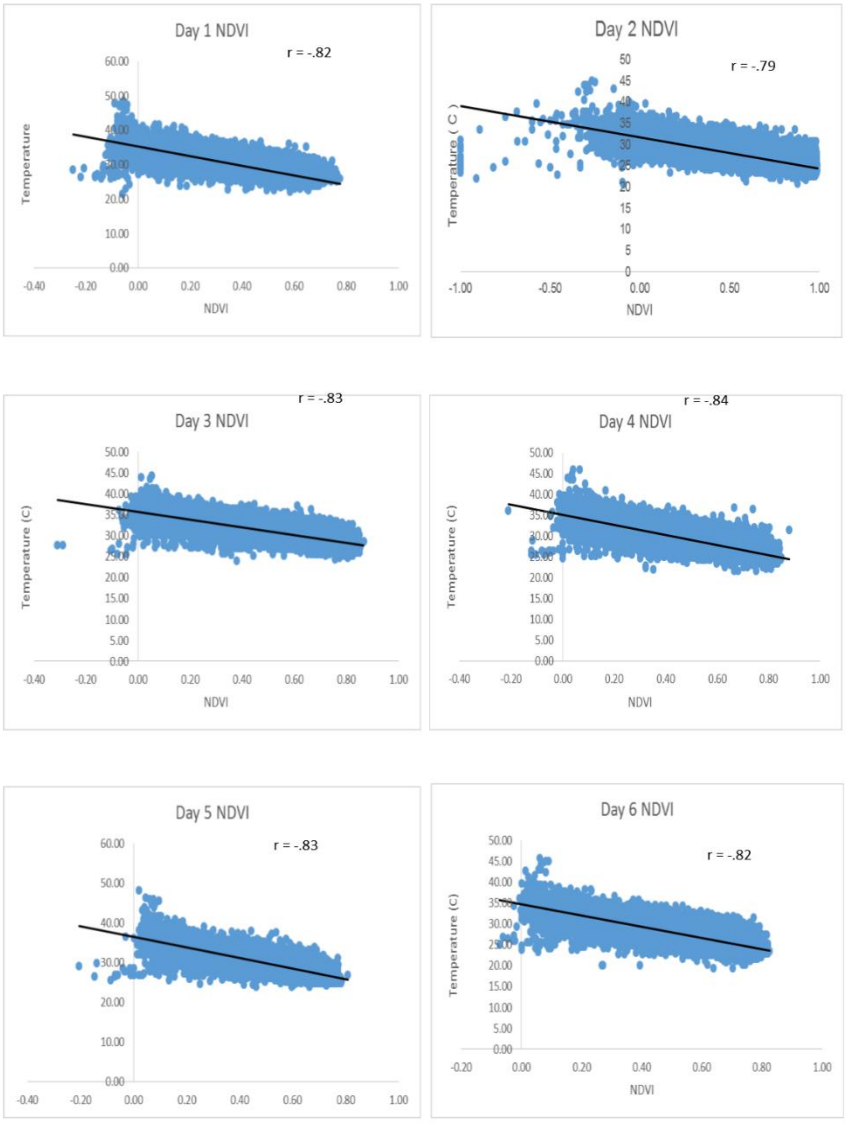

Figure 16 Scatterplots of NDVI and LST

4.4 Relationship between land surface temperature and impervious surfaces

Scatterplots as shown reveal a strong positive correlation between impervious surface and temperature (Figure 17). Correlations range from .79 to .81 indicating that as the amount of impervious surfaces increase, temperatures tend to rise.

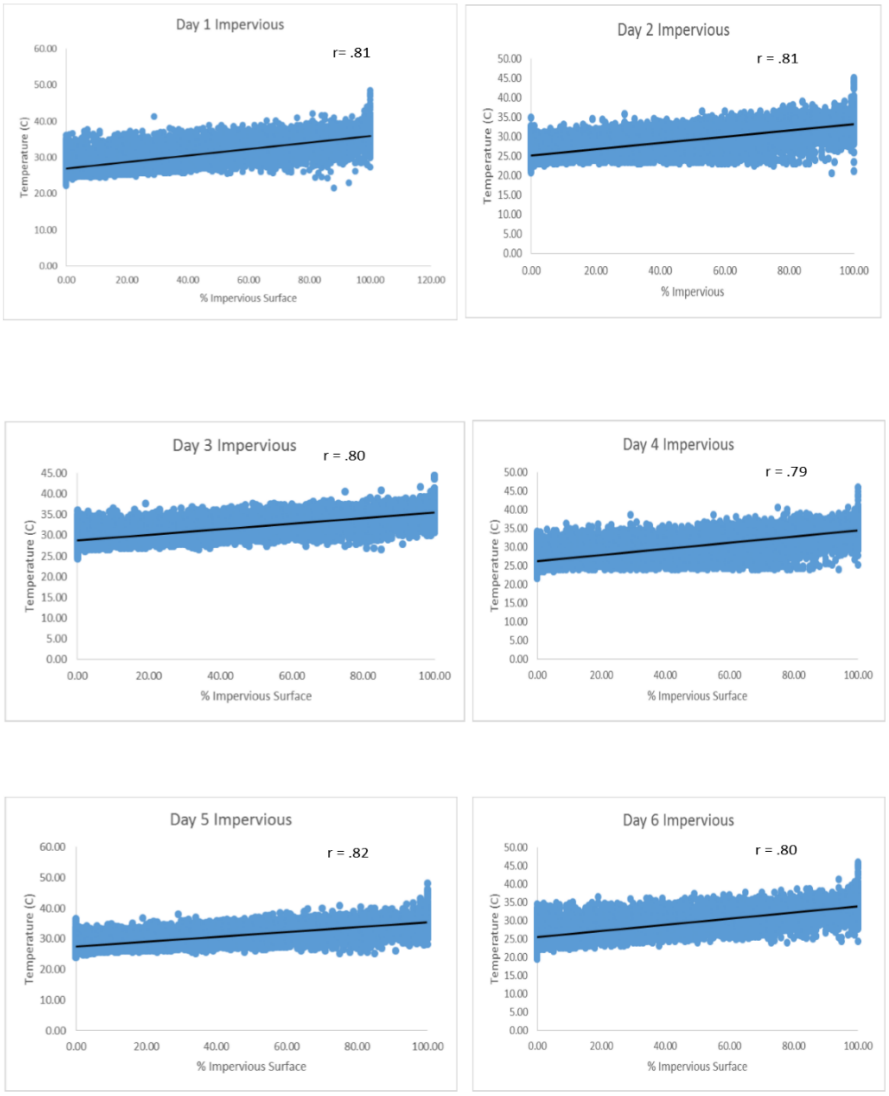

Figure 17 Impervious Surface Scatterplots

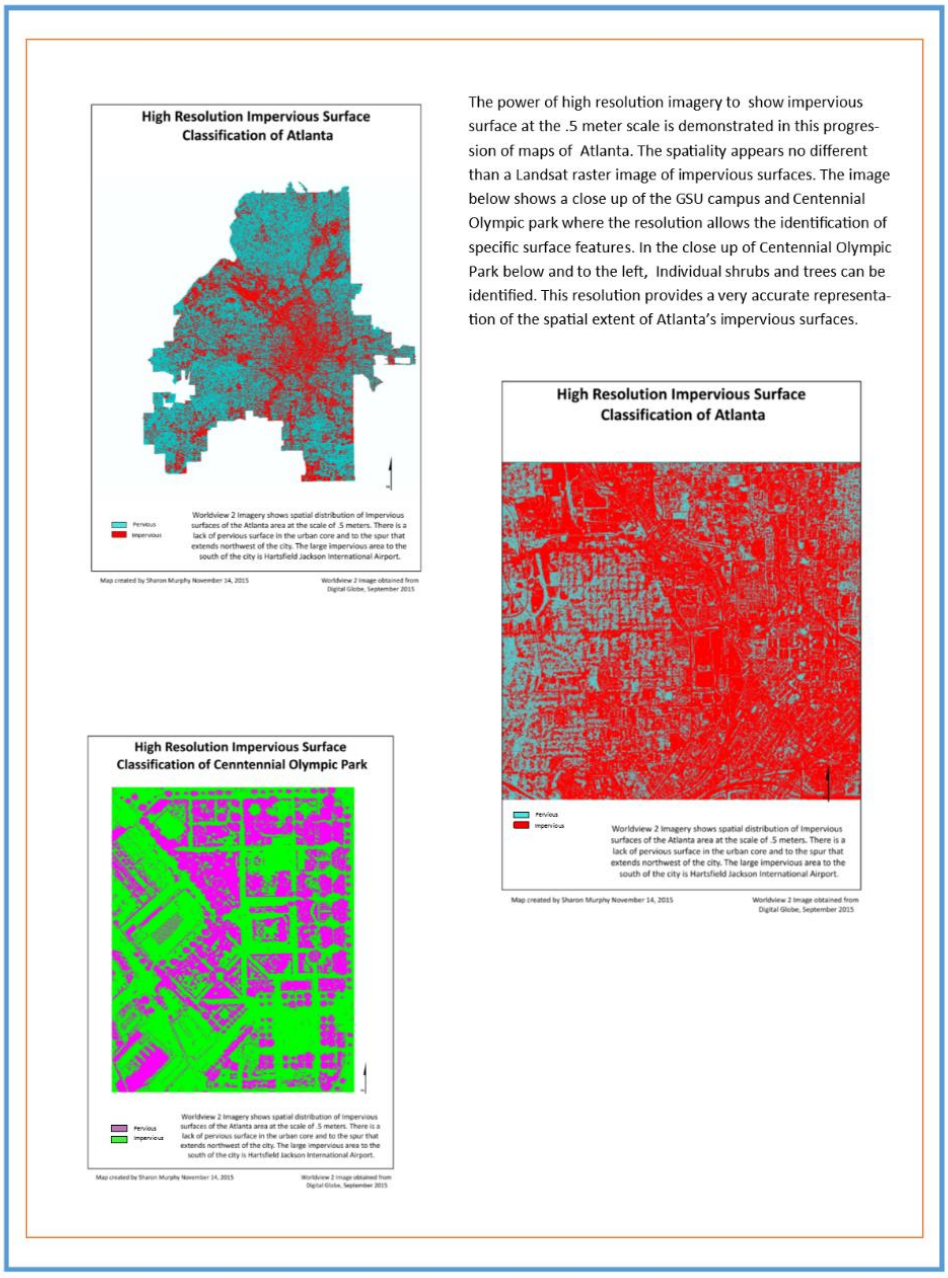

Figure 18 High Resolution of Atlanta and a Buffer Region

Figure 18 shows the result of a high resolution impervious surface analysis of Atlanta at the different scales: City, downtown, and Centennial Olympic Park. Technical parameters prevented the processing of the NDVI image at the NPU scale.

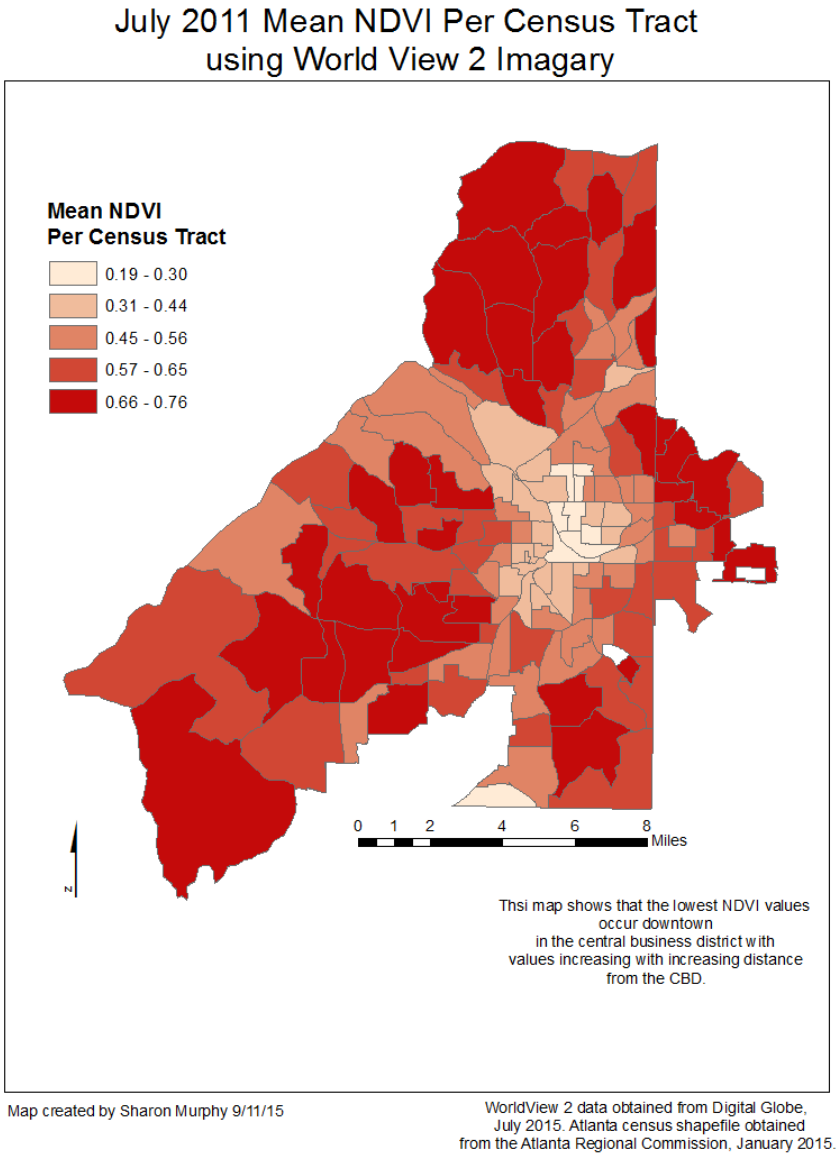

Figure 19 High Resolution Mean NDVI of Atlanta Per Census Tract

At the GSU campus scale, high resolution imagery analysis for impervious surface and NDVI in figure 20 shows the extent of impervious surface and vegetation. It is easy to visually determine that the GSU campus is largely impervious surface and lacks vegetative cover. The high resolution impervious surface classification had a strong 89% accuracy rate.

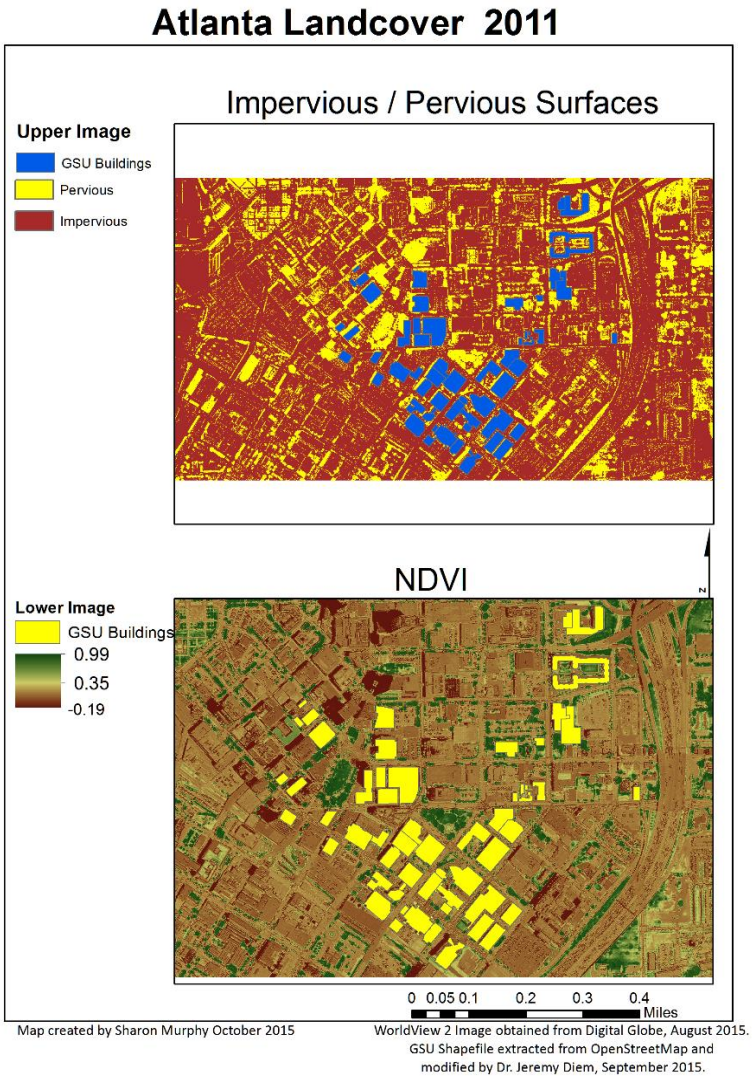

Figure 20 High resolution analysis of Impervious Surface and NDVI for the GSU Campus

4.5 Potential impacts of extensive green roofs on Atlanta's surface temperature

The re-introduction of vegetation and subsequent reduction in impervious surfaces by the addition of green roofs resulted in a 1.59° C reduction in LST at the city scale if 100% of roofs over 14,400m^2 were vegetated (Figure 21). The temperature decreases linearly with an increase

in green roof coverage. This means that installing green roof technology may have a significant impact on the urban heat island.

Mean Temperature (C) of the City of Atlanta						
% Atlanta Green Roof	Day 1	Day 2	Day 3	Day 4	Day 5	Day 6
0	29.53	27.46	30.73	28.55	29.71	27.90
10	29.35	27.28	30.55	28.37	29.53	27.72
20	29.17	27.16	30.39	28.23	29.35	27.58
50	28.63	26.71	29.87	27.74	28.82	27.10
100	27.73	25.96	29.02	26.92	27.93	26.31
Temperature of a Green roof at 11a.m.						
	Day 1	Day 2	Day 3	Day 4	Day 5	Day 6
	18.85	15.87	17.94	17.14	18.64	16.74
Temperature Change (C) from the Mean						
% Atlanta Green Roof	Day 1	Day 2	Day 3	Day 4	Day 5	Day 6
0	0.00	0.00	0.00	0.00	0.00	0.00
10	-0.18	-0.18	-0.18	-0.18	-0.18	-0.18
20	-0.36	-0.30	-0.34	-0.33	-0.36	-0.32
50	-0.90	-0.75	-0.85	-0.81	-0.89	-0.79
100	-1.80	-1.50	-1.71	-1.63	-1.78	-1.59

Figure 21 Impact on Land Surface Temperature Due to Green Roofs at the City Scale

At the scale of the GSU campus, the same analysis reveals a markedly different result. If 100% of GSU roofs were vegetated then the LST reduction increased to 2.62°C (Figure 22).

Mean Temperature (C) of the GSU Campus						
% GSU Green Roof	Day 1	Day 2	Day 3	Day 4	Day 5	Day 6
0	35.60	35.30	33.20	34.20	35.60	33.70
10	35.30	35.05	32.92	33.93	35.31	33.44
20	35.01	34.80	32.64	33.66	35.01	33.18
50	34.12	34.06	31.79	32.86	34.13	32.39
100	32.63	32.82	30.38	31.51	32.67	31.08
Temperature of Green Roof at 11 A.M.						
	Day 1	Day 2	Day 3	Day 4	Day 5	Day 6
	18.85	15.87	17.94	17.14	18.64	16.74
Temperature Change (C) From the Mean						
% GSU Green Roof	Day 1	Day 2	Day 3	Day 4	Day 5	Day 6
0	0.00	0.00	0.00	0.00	0.00	0.00
10	-0.30	-0.25	-0.28	-0.27	-0.29	-0.26
20	-0.59	-0.50	-0.56	-0.54	-0.59	-0.52
50	-1.49	-1.24	-1.41	-1.34	-1.47	-1.31
100	-2.97	-2.48	-2.82	-2.69	-2.93	-2.62

Figure 22 Impact on Land Surface Temperature Due to Green Roofs at the GSU Campus Scale

4.6 Pollutant Removal

Green roofs are an effective way to increase the atmospheric pollutant rate in an urban setting at both the city scale and the campus scale in absolute terms. The pollutant removal for the city of Atlanta revealed that green roofs would make a small impact on the overall amount of pollution removal rate that is currently taking place.

ANNUAL POLLUTANT REMOVAL (mt) ATLANTA					
% ATL Green Roof	SO_2	NO_2	PM_{10}	O_3	Total (mt)
10	2.40	8.61	4.14	16.59	317.48
20	4.80	17.22	8.28	33.19	63.50
50	12.01	430.57	20.70	82.97	158.74
100	24.02	861.14	41.39	165.94	317.48
Current Scenario	1,925.58	6,819.60	400.72	1,361.87	10,507.77
% ATL Green Roof	Percentage Increase in Removal Due to Green Roofs				
10	0.12	0.13	1.03	1.22	
20	0.25	0.25	2.07	2.44	
50	0.62	6.31	5.16	6.09	
100	1.25	12.63	10.33	12.19	

Figure 23 Annual Pollutant Removal Rates for the city of Atlanta

Figure 23 shows that even at a rate of 100% vegetated roofs for the entire city, green roofs would only increase atmospheric pollution removal by a maximum of about 12%.

An analysis of species performance in pollution removal reveals a significant difference in the ability of different plant species to remove PM_{10} from the atmosphere. Sedums proved to be a poor performer in relation to Fescue rubra (Figure 24).

Sedum album

P. lanceolata

F. rubra

A. stolinifera

ANNUAL PM_{10} REMOVAL (mt) ATLANTA				
	SEDUM	GRASSES		
% ATL Green Roofs	Sedum album	P. lanceolata	F. rubra	A. stolinifera
10	1.55	1.81	11.86	6.69
20	3.10	3.62	23.73	13.38
50	7.76	9.05	59.32	33.45
100	15.52	18.11	118.64	66.90

Figure 24 Species Level Analysis of PM10 Removal

However, at the scale of the GSU campus the results are much more dramatic. Using the GSU campus footprint, the landcover analysis revealed that the GSU campus consists of 91% impervious surface (Figure 25).

The rates for pollutant removal for the GSU campus were based off the results of this analysis and reveal a striking increase in the amount of pollutant removal due to the presence of

green roofs. If 100% of the GSU roof area were to be vegetated than a striking 70% - 75.34% increase in atmospheric pollutant removal is predicted.

ANNUAL POLLUTANT REMOVAL (kg) GSU CAMPUS					
% GSU Green Roof	SO_2	NO_2	PM_{10}	O_3	Total (kg)
10	8.57	30.72	14.77	59.20	113.26
20	17.14	61.44	29.53	118.40	226.52
50	42.85	153.61	73.84	296.01	566.30
100	85.70	307.21	147.67	592.01	1,132.61
Current	115.12	407.77	210.89	805.86	1,539.64
%GSU Green Roof	Percentage Increase in Removal Due to Green Roofs				
10	7.44	7.53	7.00	7.35	
20	14.89	15.07	14.00	14.69	
50	37.22	37.67	35.01	36.73	
100	74.45	75.34	70.02	73.46	

Figure 25 Annual Pollutant Removal at the GSU Campus Scale

With 100% of roofs at GSU vegetated with S. album, only 55.38 kg of PM10 would be removed compared with 423.24 kg that could be removed by F. rubra (Figure 26).


Sedum album


P. lanceolata


A. stolinifera


F. rubra

ANNUAL PM_{10} REMOVAL (kg)				
	SEDUM	GRASSES		
% GSU Green Roofs	Sedum album	P. lanceolata	F. rubra	A. stolinifera
10	5.54	6.46	42.32	23.87
20	11.08	12.92	84.65	47.73
50	27.69	32.30	211.62	119.33
100	55.38	64.61	423.24	238.65

Figure 26 Species Level PM10 Removal - GSU Campus Scale

4.7 Stormwater Runoff

Traditional urban development practices result in a high level of impervious surfaces that direct stormwater directly into municipal sewer systems. This results in approximately 41,269,808,992 gallons of stormwater runoff annually from all impervious surfaces, taking a 12% evaporation rate into account. Green roofs can mitigate anywhere from .06% - 3% of this run off depending on the depth of the growing medium, reducing total stormwater runoff by

approximately 275,438,102 - 1,400,143,687 gallons annually if 100% of Atlanta roofs are green roofs based on 49.58 inches of precipitation annually (Table 3).

Table 3 Runoff Scenarios for City of Atlanta

Runoff in Inches		
% ATL Green Roof	2 Inches Growing Medium	8 Inches Growing Medium
0	17.98	17.98
10	17.97	17.92
20	17.95	17.86
50	17.92	17.67
100	17.86	17.37
Runoff in Gallons for Atlanta (3,679,867,766 square feet)		
% ATL Green Roof	2 Inches Growing Medium	8 Inches Growing Medium
0	41,269,808,992.38	41,269,808,992.38
10	41,246,855,817.19	41,132,089,941.24
20	41,200,949,466.81	40,994,370,890.10
50	41,132,089,941.24	40,558,260,561.48
100	40,994,370,890.10	39,869,665,305.77
Change in Runoff from Current Situation		
% ATL Green Roof	2 Inches Growing Medium	8 Inches Growing Medium
0	0.00	0.00
10	-22,953,175.19	-137,719,051.14
20	-68,859,525.57	-275,438,102.29
50	-137,719,051.14	-711,548,430.90
100	-275,438,102.29	-1,400,143,686.62
% Change in Runoff for all of Atlanta		
% ATL Green Roof	2 Inch Growing Medium	8 Inch Growing Medium
0	0.00	0.00
10	-0.06	-0.33
20	-0.17	-0.67
50	-0.33	-1.72
100	-0.67	-3.39

At the GSU campus scale, the reduction in stormwater runoff is much more dramatic. If 100% of GSU roofs were vegetated, the runoff reduction increased by32.3% (Table 4).

Table 4 Runoff Scenarios for the Campus of Georgia State University

Runoff in Inches		
% Roofs that are Green	2 Inch Growth Media	8 Inch Growth Media
0	39.82	39.82
10	39.57	38.46
20	39.31	37.09
50	38.55	32.99
100	37.51	26.96
Runoff in Gallons for GSU footprint (8,479,873 square feet)		
% Roofs that are Green	2 Inch Growth Media	8 Inch Growth Media
0	210,620,754	210,620,754
10	209,298,423	203,427,277
20	207,923,200	196,180,908
50	203,903,316	174,494,693
100	198,402,423	142,600,088
Change in Runoff from Current Situation		
% Roofs that are Green	2 Inch Growth Media	8 Inch Growth Media
0	0	0
10	-1,322,330	-7,193,476
20	-2,697,554	-14,439,846
50	-6,717,437	-36,126,061
100	-12,218,331	-68,020,665
% Change in Runoff for the GSU Footprint		
% Roofs that are Green	2 Inch Growth Media	8 Inch Growth Media
0	0.00	0.00
10	-0.63	-3.42
20	-1.28	-6.86
50	-3.19	-17.15
100	-5.80	-32.30

In an undisturbed state, runoff is estimated to be about .67% or 1,537,862,738 gallons annually assuming a landcover composition of 80% forest and 20% meadow. Table 5 shows that when the percentage of stormwater runoff for various green roof scenarios takes predicted climate change trends into account that the increase in runoff is modest.

Table 5 Stormwater Runoff by Percentage for Climate Change Scenarios

Percentage of Stormwater Runoff

For Different Green Roof Scenarios in Atlanta

Depth of Growing Medium (inches)	Present Day	Near Term Climate Change	Far Term Climate Change
2	81	81	82
4	70	71	72
6	62	63	64
8	56	57	58
Conventional Roof	88	89	90
Natural State	2 – 23	2 - 25	3 - 26

The hydrological structure of Atlanta is comprised of a series of small watersheds that primarily feed into two larger river basins: the Apalachicola, Flint, and Chattahoochee River Basin (ACF) and the Ocmulgee River Basin. The ACF River Basin drains into the Gulf of Mexico, while the Ocmulgee River Basin drains into the Atlantic Ocean. The GSU campus spans two watersheds, the Proctor Creek Watershed and the Intrenchment Creek Watershed. Since our

study area focuses on the GSU Sports Arena specifically, the path of the stormwater runoff from that location will be analyzed closely. Stormwater from this location is directed to the Intrenchment Creek Watershed where it is transported to through the South River Watershed to the South River Wastewater Treatment Facility as shown in Figure 27.

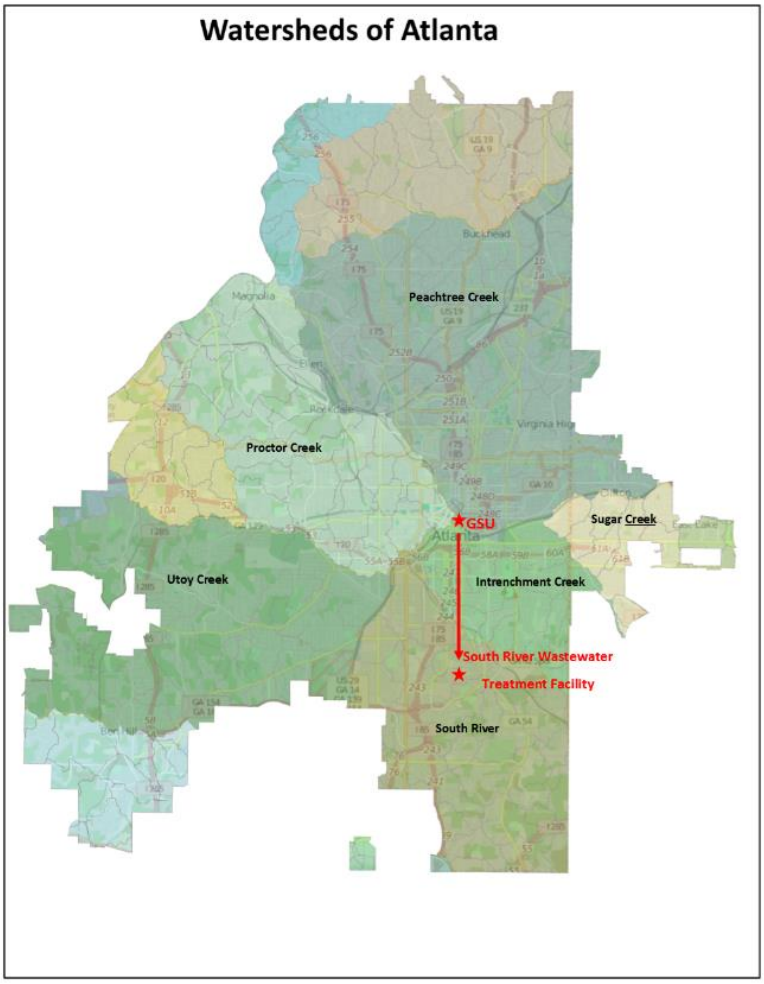

Figure 27 Watersheds of Atlanta

The Intrenchment Creek and South River Watersheds are part of the Ocmulgee River Basin which naturally drains to the Atlantic Ocean as shown in Figure 28.

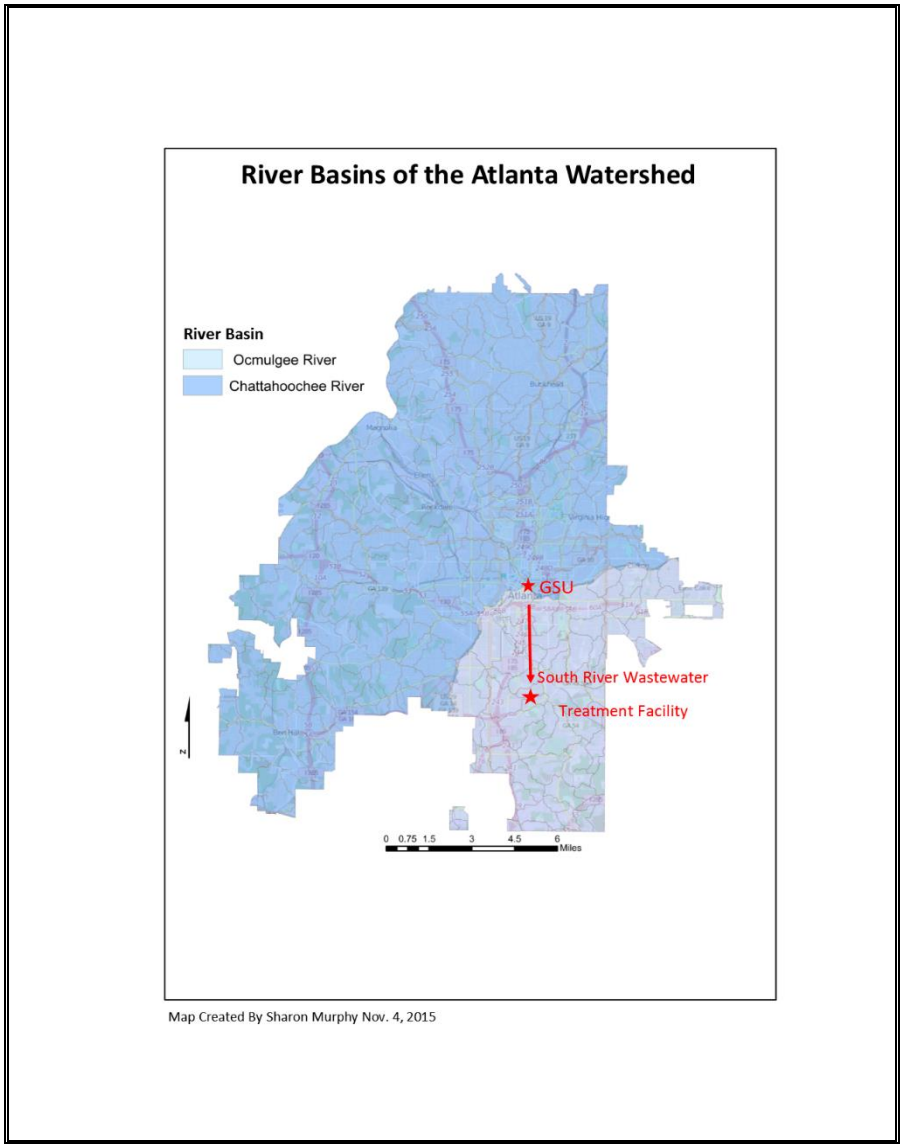

Figure 28 Atlanta River Basins

However, the city of Atlanta Department of Watershed Management diverts this water to the Chattahoochee River (ACF River Basin) after processing. Eventually the stormwater from

the GSU Sports Arena ends up in the Gulf of Mexico instead of the Atlantic where it would naturally drain (Figure 29).

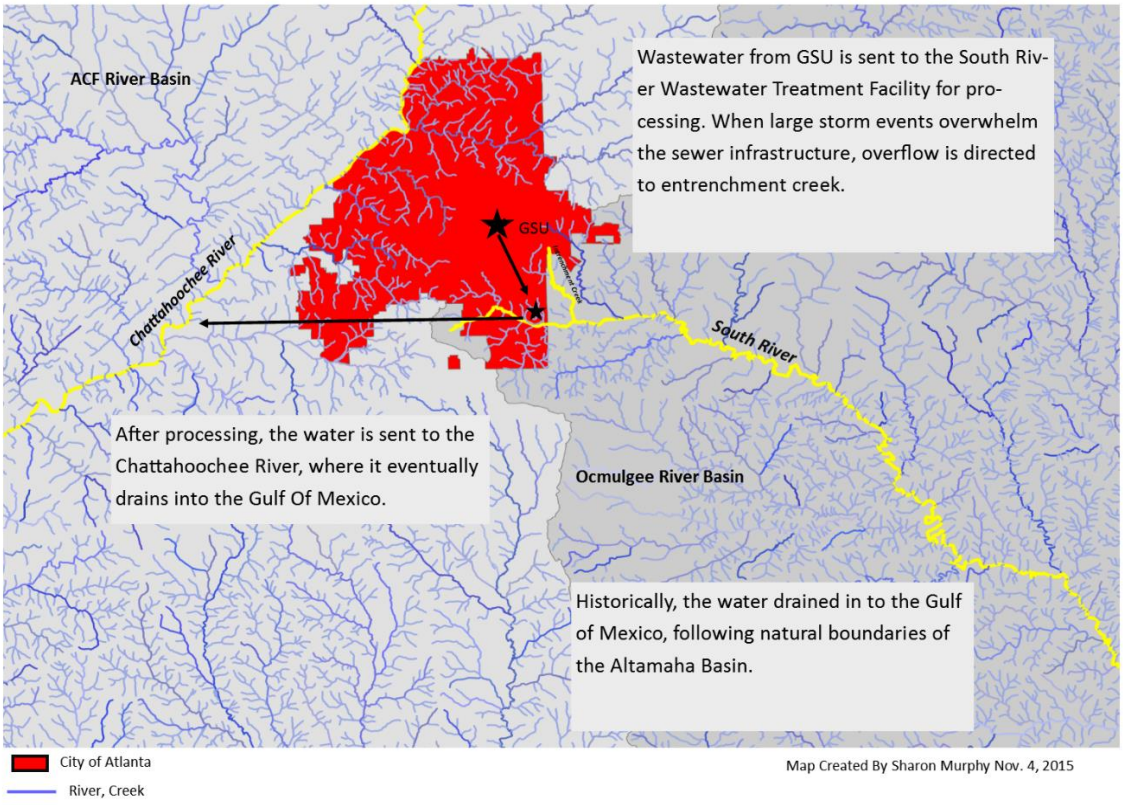

Figure 29 GSU Stormwater Path

5 DISCUSSION

5.1 The Influence of Green Roofs on the Urban Heat Island in Atlanta and GSU

With urban areas experiencing a greater increase in minimum daily temperatures than their rural surroundings due to climate change, it is expected that EHE related mortality will also increase. In addition to mortality, the increasing temperatures will also

increase energy consumption as cooling systems work harder and longer to keep buildings as comfortable as possible. A by-product of operating a cooling system is that they produce heat as a result of mechanical processes, which compounds the urban heat island effect that they are working to offset. The warmer the climate, the harder a system must work to cool a building and therefore the more heat it produces in an effort to cool that building. 'Process' heat in conjunction with the built environment emitting longwave radiation prevents the urban core from cooling down at night, thereby increasing the risk for EHE related mortality.

The correlation between impervious surface and temperature is near perfect at .979. This can be confirmed visually as the map in figure 7 shows that the warmest area of Atlanta is the urban core, followed by major thoroughfares that are lined with commercial industry. Roads are typically constructed of dark asphalt, and the commercial areas normally consist of asphalt parking lots and buildings with dark roofs. This type of built environment is largely made of impervious surfaces so there is no surprise that they are also the warmest areas of the city. Conversely, the coolest areas of Atlanta are those areas with a low percentage of impervious surfaces and a high percentage of vegetated land. This information, combined with the knowledge that extreme heat events will be increasing in both magnitude and duration, mean the areas of Atlanta that are most vulnerable to heat events can be identified as those with the greatest amount of impervious surfaces.

The urban core, with its high percentage of impervious surfaces and low percentages of vegetated space has the highest mean temperature of the metro Atlanta area. Two other locations were identified as having extremely high land surface temperatures; one

location being an extremely large server farm, and the other location being a glass production factory. However, both of these points lie outside of the urban core and their temperature influence is localized.

GSU has been largely responsible for the revitalization of the urban core of Atlanta. As the fastest growing university in the University of Georgia System, GSU is responsible for the surge in new residential units being built on or near campus to provide housing options for GSU students. The revitalization of the urban core has attracted business and industry to locate their operations downtown near the GSU campus. For instance, Microsoft is locating their new Innovation Center in the Flat Iron Building located adjacent to the GSU campus. This movement of people back to the urban core of Atlanta means that people are moving into the warmest part of Atlanta, which will increase the demand for air conditioning, which will produce even more heat in the process of creating cool air and exacerbating the urban heat island effect.

Knowing the correlation between impervious surface and increased land surface temperature in Atlanta is a strong .79 to .82, it follows that a reduction in impervious surfaces should reduce land surface temperatures. The results of this study show that LST can be decreased by 3°C to 2.97°C at the GSU scale depending on the area covered in vegetated roofs. Therefore, increasing the amount of vegetated, pervious surfaces in the built environment should be an effective way to mitigate the urban heat island and also help mitigate the damaging effects of an extreme heat event in Atlanta.

Another byproduct of the Atlanta UHI is the enhancement of summer storms due to the increase in convective currents and heating produced by the UHI. Maximum enhancement occurs northeast of Atlanta in Gwinnett County which is located about 17

miles northeast of Atlanta (Diem, 2008). If the UHI effect were minimized, it is possible that summer storm enhancement would be reduced which would be an indirect benefit of instituting green roof technology.

5.2 The Influence of Green Roofs on Pollutants in Atlanta and at GSU

Rooftops present a challenge for successfully growing vegetation due to the harsh conditions that occur with changes in elevation. Raising the elevation increases the plants exposure to solar radiation and wind and care must be taken to select plants that are able to tolerate these conditions. Sedums are a popular choice for extensive green roofs because they are drought, wind, and, depending on the cultivar, sun tolerant. Sedums are succulents, specifically they are part of the family of succulents that use crassulacean acid metabolism (CAM4) which is an adaptation that allows them to tolerate arid conditions. While sedums are very good at tolerating arid conditions, they are not as efficient at reducing the surface temperature of a green roof as grasses are (Lundholm, MacIvor, MacDougall, & Ranalli, 2010) and therefore are not the best vegetation choice if environmental benefits are the primary concern.

Grasses, especially native grasses, are extremely efficient at cooling the surface of the roof and removing PM_{10} due to their structure and biomass. The limiting factor for grasses is that they do need a deeper growing medium than sedums and more irrigation days in order to thrive, and therefore require a greater structural load capacity from the building. However, the deeper growing medium and the need for irrigation mean a green roof of grasses is more effective at cooling because of active evapotranspiration processes and superior energy partitioning (Santamouris, 2014). Typical growing mediums for green roof vegetation follows FLL guidelines (green roof industry guidelines) that requires 80% inorganic matter and 20% organic

matter for growing mediums. This composition results in a porous structure that allows more air pockets than what is found in typical soils. A greater amount of air in the growing medium means there is less thermal conductivity due to the resultant lack of soil moisture which reduces heat transmission, lowering the cooling potential of the green roof (Nardini, Andri, & Crasso, 2012).

The amounts of pollutants that could be removed from the atmosphere by vegetated roofs is likely to be an overestimate. Factors such as the size and structure of the plant, as well as the species play a large role in determining the effectiveness of pollutant removal by a green roof. Some plant species emit biogenic volatile organic compounds to a greater degree than other plant species. For instance, the process of ozone formation is not linear and depends upon the presence of UV radiation and NOx in order to produce ozone. However, the presence of NO_2 also inhibits the production of ozone. OH and NO_3 radicals oxidize hydrocarbons (VOC's) into peroxyacyl and hydroperoxyacl that react with NO and turn it into NO_2. In the presence of UV radiation, NO_2 becomes O_3. However, O_3 reacts with NO to produce NO_2 again which reduces the availability of OH radicals for hydrocarbon oxidation by forming NHO_3, meaning that a decrease in NO leads to an increase in O_3. This balance between the production of ozone and the availability of NOx determines the level of effectiveness that a green roof will have in removing ozone from the atmosphere (Hewitt, 1999). Fernando (2001) states that surface level pollutants remain at the surface level until they are forced into the atmospheric boundary level by convective or turbulent mixing. The increasing of surface roughness by the addition of vegetation can generate shear turbulence up to 2-3 times the height of the vegetative canopy, increasing the mixing and dispersion of pollutants including ozone and its precursors. The benefit of ozone removal from the atmosphere via wet and dry deposition versus the addition of

ozone precursors to the atmosphere, coupled with atmospheric mixing generated by a vegetative surface is something that is highly dependent upon the species and size of plants that the vegetated roof consists of.

5.3 The Influence of Green Roofs on Stormwater Runoff in Atlanta and at GSU

The results of this study show that shallow, extensive green roofs have a limited ability to mitigate stormwater runoff. An annual reduction of 3% of stormwater runoff for the entire city of Atlanta if all roofs were vegetated is a modest benefit. Considering the age of the buildings in Atlanta and their accessibility, a large portion of rooftops would not be good candidates for greening. Therefore, even a 3% reduction in stormwater runoff is unrealistic. However, at the GSU scale with its large expanse of impervious surfaces, stormwater runoff can be reduces by as much as 32.3% if all roofs were vegetated. Again, this scenario is unrealistic but it does demonstrate the impact that increasing vegetated spaces can have when the built environment consists of 91% impervious surfaces.

Total stormwater runoff mitigation is just one metric for measuring the impact vegetated roofs have on stormwater runoff. A study that modeled the impact different green roof scenarios could have during differing degrees of precipitation events found that green roofs would be effective at reducing peak attenuation of runoff. The degree of attenuation modification depended on the green roof configuration and the size of the storm event (Polinsky, 2009). Since 75% of all impervious surfaces in Atlanta are roads and parking lots, stormwater mitigation strategies at ground level will have a greater impact than green roofs do. Incorporating bioswales and raingardens into public landscape designs, and using pervious pavements in

addition to green roofs are strategies that are increasingly being used by municipalities to control stormwater runoff.

Given the modest decrease in total stormwater runoff from the installation of vegetated roofs, can flooding at the city or basin scale be alleviated by green roof technology? The combined sewer overflow system of the city of Atlanta can become overwhelmed during very large precipitation events causing raw sewage to be discharged into area streams. By reducing peak attenuation and total runoff, Versini et al (2015) found that 35% area coverage with green roofs can prevent some flooding issues at both the city and basin scale. However, the results of the impact green roofs have at the basin scale depend on the potential that the land cover the basin is comprised of for the installation of green roofs. It may make more sense to study the downstream impact of green roofs at a smaller scale such as the watershed scale where deleterious storm effects can be directly related to changes in urban landcover. As the results of this study show, the impact on stormwater runoff is the greatest at the GSU scale where the greatest amount of impervious surface exists, therefore focusing on the impact of green roofs on the potential to mitigate downstream flooding at the watershed scale could be valuable.

Because of the dynamic nature of the atmosphere, sophisticated modeling beyond the scope of this study is needed in order to determine the extent wide deployment of green roof technology could offset the urban heat island phenomenon. Fernando (2001) has found that the orientation of the built environment to the prevailing winds, as well as distance between buildings and their heights influence the behavior of the urban canopy layer and the ability of wind to penetrate the urban core at street level. Buyantuyev & Wu (2010) found that the addition of a green roof reduces the depth of the planetary boundary layer which has the potential to increase the perception of decreased air quality. Fernando (2001) also found that green roofs increase surface

roughness thereby causing an increase in convective mixing in the lower levels of the atmosphere, possibly causing the perception of air quality increasing. The amount of surface roughness created by a green roof depends on the type of green roof is being studied, with an intensive green roof increasing surface roughness and an extensive green roof having less of an effect on surface roughness(Peng, 2012). Each of these characteristics contributes to determining the ambient air temperature but the combination of vector processes (wind) which has both magnitude and direction, and scalar data (temperature) which has magnitude only makes it difficult to predict how green roofs will impact ambient temperature.

This study found significant reductions in the LST at the GSU scale with modest reductions at the Atlanta scale. This is likely due to the large amount of vegetated surfaces at the Atlanta scale and the lack of vegetated surfaces at the GSU scale. Studies modeling the effect of widespread deployment of green roof technology are limited by the fact urban atmosphere-biosphere coupling is a complex process that is confounded by the form and composition of the built environment. Therefore, extrapolating the LST results of this study to changes in ambient air temperature is not recommended.

The International Panel on Climate Change (IPCC) models predict that precipitation will increase by 5% as global temperatures rise due to the resultant increase in atmospheric water vapor. An increase of precipitation on a sewer system already burdened at the current precipitation rate will likely increase the number and magnitude of sewer overflow events. It becomes even more important to control as much stormwater as possible before it enters the municipal sewer system under this scenario. Green roofs can be a significant aspect of stormwater mitigation strategies, especially as the depth of growing medium deepens.

However, in an urban area where new construction is limited, retrofitting an older building for a green roof can be expensive. The typical barriers that prevent the adoption of green roof technology are listed in Table eight. Many existing urban buildings encounter all of the listed barriers making adoption of green roof technology less likely. New construction is the best candidate for the installation of a green roof because many of the barriers can be overcome at the design phase of the construction process.

Table 6 Barrier and Benefits to Green Roof Adoption

Green Roof Benefits	Green Roof Barriers
Reduced Energy Use	Higher cost of installation as opposed to a conventional roof
Increased thermal insulation reduces rooftop heat flux	May require weeding and irrigation, especially when new
Extends life of the roof by ~20 yrs	Installation requires specialized knowledge in green roof construction, horticulture, and
Reduces storm water run off, helping to reduce sewer system overflows.	May fail if not installed or maintained properly
Qualifies for LEED credits	If roof load capacity is insufficient then reinforcing the roof can be expensive .
Turns non-functional space into functional space	Access points to roof may not be suitable
Removes pollutants from the air and from storm water runoff	HVAC and venting systems may infringe on the roof space ina way that makes the space unusable

Examples of Green Roof Incentives

Austin, TX - Green Roof Density Bonus gives building entitlements beyond what zoning offers if construction offers benefits to the community.

Chicago, IL— If a green roof covers 2,000 sq. ft. or 50% of the roof area then builder is eligible for a Floor Area Ratio Bonus. Chicago also offers expedited permitting to developers incorporating green building techniques as outlined by the United States Green Building Council.

Los Angeles, CA —Building projects larger than 7500 sq. ft. are required to meet LEED standards.

Maryland— Stormwater management credits up to $10,000 for property owners that install approved stormwater management controls.

Milwaukee, WI—The Green Roof Initiative provides up to $5 per sq. ft. For an approved green roof project.

Nashville, TN—Promotes the installation of green roofs by giving a $10 credit in a property's sewer fees for every square foot of green roof installed.

New York City—The NYC Department of Buildings provides up to $5.23 rebate per square foot for a green roof installation, up to a maximum of $200,000.

Philadelphia, PA—Tax credit of 25% of the cost of green roof installation up to a maximum of $100,00.

Portland, OR—FAR Bonus of an extra 3sq. ft. per 1 sq. ft. of green roof, plus reimbursement of $5 sq. ft. for stormwater management, and $5 sq. ft. through the Grey to Green initiative for a total of $10 per sq. ft.

San Francisco, CA—Low rate loans and longer terms for properties installing green roofs, as well as expedited permitting process.

6 Study Limitations

The primary limitation of this study is the coarse resolution of the thermal band of the Landsat 5 images that were used to determine the spatiality of heat distribution in Atlanta. At $120m^2$ per pixel, it is impossible to definitively state what the land surface temperature is at any point in the metro region. It is possible to draw conclusions based on the relative distribution of temperature at the city scale from this study, but not to state the exact extent temperature differs from one point to the next. This study is also limited by the lack of data that pertains specifically to the city of Atlanta with regards to green roof studies. There are opportunities for research into the impacts that green roofs could have on the city of Atlanta should a green roof be installed on the campus. These studies would help inform public policy as it relates to growth and development in the face of a warming climate.

7 Conclusion

The urban heat island effect is closely correlated with the loss of pervious and vegetated surfaces in the urban area. In Atlanta, the urban core has been shown to be the warmest area of the metro area and it also has the least amount of pervious and vegetated surfaces in the metro area. The high correlation between impervious surface and land surface temperature in Atlanta is in agreement with the majority of peer reviewed literature and can confidently be used as the best predictor of land surface temperature distribution in Atlanta.

The presence of a green roof on the GSU campus would offer several benefits including pollution abatement, on-site stormwater management, and urban heat island mitigation. The scale at which green roofs would need to be deployed in order to offset the negative environmental impacts of urbanization depends upon where the green roofs are located. The

impact at the GSU scale is much greater than the impact at the Atlanta scale due to the abundance of vegetated spaces at the city scale and the lack of vegetated spaces at the campus scale. Strategically placing green roofs at the urban core will significantly affect stormwater runoff, air quality, and the UHI in Atlanta.

REFERENCES

Akbari, H., Pomerantz, M., & Taha, H. (2001). Cool surfaces and shade trees to reduce energy use and improve air quality in urban areas. *Solar Energy*, *70*(3), 295–310. http://doi.org/10.1016/S0038-092X(00)00089-X

Alexander, L. (2011). Climate science: Extreme heat rooted in dry soils. *Nature Geoscience*, *4*(1), 12–13. http://doi.org/10.1038/ngeo1045

Alexander, L. V., Zhang, X., Peterson, T. C., Caesar, J., Gleason, B., Klein Tank, A. M. G., … Vazquez-Aguirre, J. L. (2006). Global observed changes in daily climate extremes of temperature and precipitation. *Journal of Geophysical Research*, *111*(D5). http://doi.org/10.1029/2005JD006290

Amengual, A., Homar, V., Romero, R., Brooks, H. E., Ramis, C., Gordaliza, M., & Alonso, S. (2014). Projections of heat waves with high impact on human health in Europe. *Global and Planetary Change*, *119*, 71–84. http://doi.org/10.1016/j.gloplacha.2014.05.006

Anderson, G. B., & Bell, M. L. (2010). Heat Waves in the United States: Mortality Risk during Heat Waves and Effect Modification by Heat Wave Characteristics in 43 U.S. Communities. *Environmental Health Perspectives*, *119*(2), 210–218. http://doi.org/10.1289/ehp.1002313

Anderson, J., Fernando, H. J. S., Lee, S. M., Grossman-Clarke, S., Pardyjak, E., & Princevac, M. (2001). Urban fluid mechanics: air circulation and contaminant dispersion incities. *Environmental Fluid Mechanics*, *1*(1), 107.

Barsi, J. A., Hook, S. J., Schott, J. R., Raqueno, N. G., & Markham, B. L. (2007). Landsat-5 Thematic Mapper Thermal Band Calibration Update. *IEEE Geoscience and Remote Sensing Letters*, *4*(4), 552–555. http://doi.org/10.1109/LGRS.2007.896322

Buyantuyev, A., & Wu, J. (2010). Urban heat islands and landscape heterogeneity: linking spatiotemporal variations in surface temperatures to land-cover and socioeconomic patterns. *Landscape Ecology*, *25*(1), 17–33. http://doi.org/10.1007/s10980-009-9402-4

Calderón-Garcidueñas, L., Calderón-Garcidueñas, A., Torres-Jardón, R., Avila-Ramírez, J., Kulesza, R. J., & Angiulli, A. D. (2015). Air pollution and your brain: what do you need to know right now. *Primary Health Care Research & Development*, *16*(04), 329–345. http://doi.org/10.1017/S146342361400036X

Calderón-Garcidueñas, L., & Torres-Jardón, R. (2012). Air pollution, socioeconomic status, and children's cognition in megacities: the Mexico City scenario. *Frontiers in Psychology*, *3*, 1–4. http://doi.org/10.3389/fpsyg.2012.00217

Chen, X.-L., Zhao, H.-M., Li, P.-X., & Yin, Z.-Y. (2006). Remote sensing image-based analysis of the relationship between urban heat island and land use/cover changes. *Remote Sensing of Environment*, *104*(2), 133–146. http://doi.org/10.1016/j.rse.2005.11.016

Churkina, G., Grote, R., Butler, T. M., & Lawrence, M. (2015). Natural selection? Picking the right trees for urban greening. *Environmental Science & Policy*, *47*, 12–17. http://doi.org/10.1016/j.envsci.2014.10.014

Clark, C., Adriaens, P., & Talbot, F. (2008). Green roof valuation: A probabilistic economic analysis of environmental benefits. *ENVIRONMENTAL SCIENCE & TECHNOLOGY*, *42*(6), 2155–2161.

Coseo, P., & Larsen, L. (2014). How factors of land use/land cover, building configuration, and adjacent heat sources and sinks explain Urban Heat Islands in Chicago. *Landscape and Urban Planning*, *125*, 117–129. http://doi.org/10.1016/j.landurbplan.2014.02.019

Costanzo, V., Evola, G., & Marletta, L. (2015). Energy savings in buildings or UHI mitigation? Comparison between green roofs and cool roofs. *Energy and Buildings*. http://doi.org/10.1016/j.enbuild.2015.04.053

Currie, B. A., & Bass, B. (2008). Estimates of air pollution mitigation with green plants and green roofs using the UFORE model. *Urban Ecosystems*, *11*(4), 409–422. http://doi.org/10.1007/s11252-008-0054-y

Darrow, L., A., Klein, M., Strickland, M., J., Mulholland, J., A., & Tolbert, P., E. (2011). Ambient Air Pollution and Birth Weight in Full-Term Infants in Atlanta, 1994-2004. *Environmental Health Perspectives*, *119*(5), 731–737. http://doi.org/10.1289/ehp.1002785

Davis, R. E., Knappenberger, P. C., Michaels, P. J., & Novicoff, W. M. (2003). Changing Heat-Related Mortality in the United States. *Environmental Health Perspectives*, *111*(14), 1712–1718. http://doi.org/10.1289/ehp.6336

DeGaetano, A. T., & Allen, R. J. (2002). Trends in twentieth-century temperature extremes across the United States. *Journal of Climate*, *15*(22), 3188–3205. http://doi.org/10.1175/1520-0442(2002)015<3188:TITCTE>2.0.CO;2

Diem, J. E. (2008). Detecting summer rainfall enhancement within metropolitan Atlanta, Georgia USA. *International Journal of Climatology*, *28*(1), 129–133. http://doi.org/10.1002/joc.1560

Diem, J. E. (2009). Atmospheric characteristics conducive to high-ozone days in the Atlanta metropolitan area. *Atmospheric Environment*, *43*(25), 3902–3909. http://doi.org/10.1016/j.atmosenv.2009.04.050

Diem, J. E., Hursey, M. A., Morris, I. R., Murray, A. C., & Rodriguez, R. A. (2010). Upper-Level Atmospheric Circulation Patterns and Ground-Level Ozone in the Atlanta Metropolitan Area.

Journal of Applied Meteorology and Climatology, *49*(11), 2185–2196. http://doi.org/10.1175/2010JAMC2454.1

Dousset, B., & Gourmelon, F. (2003). Satellite multi-sensor data analysis of urban surface temperatures and landcover. *ISPRS Journal of Photogrammetry and Remote Sensing*, *58*(1-2), 43–54. http://doi.org/10.1016/S0924-2716(03)00016-9

Dugord, P.-A., Lauf, S., Schuster, C., & Kleinschmit, B. (2014). Land use patterns, temperature distribution, and potential heat stress risk – The case study Berlin, Germany. *Computers, Environment and Urban Systems*, *48*, 86–98. http://doi.org/10.1016/j.compenvurbsys.2014.07.005

Durre, I., Wallace, J. M., & Lettenmaier, D. P. (2000). Dependence of Extreme Daily Maximum Temperatures on Antecedent Soil Moisture in the Contiguous United States during Summer. *Journal of Climate*, *13*(14), 2641–2651. http://doi.org/10.1175/1520-0442(2000)013<2641:DOEDMT>2.0.CO;2

Dvorak, B., & Volder, A. (2013). Rooftop temperature reduction from unirrigated modular green roofs in south-central Texas. *Urban Forestry & Urban Greening*, *12*, 28–35. http://doi.org/10.1016/j.ufug.2012.05.004

Easterling, D. R. (2000). Climate Extremes: Observations, Modeling, and Impacts. *Science*, *289*(5487), 2068–2074. http://doi.org/10.1126/science.289.5487.2068

Farrugia, S., Hudson, M. D., & McCulloch, L. (2013). An evaluation of flood control and urban cooling ecosystem services delivered by urban green infrastructure. *International Journal of Biodiversity Science, Ecosystem Services & Management*, *9*(2), 136–145. http://doi.org/10.1080/21513732.2013.782342

Fischer, E. M., Seneviratne, S. I., Vidale, P. L., Lüthi, D., & Schär, C. (2007). Soil Moisture–Atmosphere Interactions during the 2003 European Summer Heat Wave. *Journal of Climate*, *20*(20), 5081–5099. http://doi.org/10.1175/JCLI4288.1

Fujii, T., & Hartshorn, T. A. (1995). The changing metropolitan structure of Atlanta, Georgia: Locations of functions and regional structure in a multinucleated urban area. *Urban Geography*, *16*(8), 680–707.

Gaffen, D. J., & Ross, R. J. (1998). Increased summertime heat stress in the US. *Nature*, *396*(6711), 529–530. http://doi.org/10.1038/25030

Gaffin, Sr., Rosenzweig, C., Eichenbaum-Pikser, J., Khanbilvardi, R., & Susca, T. (2010). A temperature and seasonal energy analysis of green, white, and black roofs. *Center for Climate Systems Research, Columbia University, New York, Technical Report No*. Retrieved from http://www.greengridroofs.com/pdf_docs/Downloads/Columbia_Energy_Analysis.pdf

Georgescu, M. (2015). Challenges Associated with Adaptation to Future Urban Expansion. *Journal of Climate*, *28*(7), 2544–2563. http://doi.org/10.1175/JCLI-D-14-00290.1

Goldberg, D. (1998). Heads up, Atlanta: it's clean air time. *Planning*, *64*(7), 20–23.

Grossman-Clarke, S., Zehnder, J. A., Loridan, T., & Grimmond, C. S. B. (2010). Contribution of Land Use Changes to Near-Surface Air Temperatures during Recent Summer Extreme Heat Events in the Phoenix Metropolitan Area. *Journal of Applied Meteorology and Climatology*, *49*(8), 1649–1664. http://doi.org/10.1175/2010JAMC2362.1

Hansen, J., Sato, M., & Ruedy, R. (2012). Perception of climate change. *Proceedings of the National Academy of Sciences*, *109*(37), E2415–E2423.

Harlan, S. L., Brazel, A. J., Prashad, L., Stefanov, W. L., & Larsen, L. (2006). Neighborhood microclimates and vulnerability to heat stress. *Social Science & Medicine*, *63*(11), 2847–2863. http://doi.org/10.1016/j.socscimed.2006.07.030

Heisler, G. M., & Brazel, A. J. (2010). The urban physical environment: Temperature and urban heat islands. *Urban Ecosystem Ecology*, (urbanecosysteme), 29–56.

Hewitt, C. N. (1999). *Reactive Hydrocarbons in the Atmosphere*. San Diego, CA: Academic Press.

Hope, D., Gries, C., Zhu, W., Fagan, W. F., Redman, C. L., Grimm, N. B., … Kinzig, A. (2003). Socioeconomics drive urban plant diversity. *Proceedings of the National Academy of Sciences*, *100*(15), 8788–8792. http://doi.org/10.1073/pnas.1537557100

Huang, G., Zhou, W., & Cadenasso, M. L. (2011). Is everyone hot in the city? Spatial pattern of land surface temperatures, land cover and neighborhood socioeconomic characteristics in Baltimore, MD. *Journal of Environmental Management*, *92*(7), 1753–1759. http://doi.org/10.1016/j.jenvman.2011.02.006

Jacquemin, B., Siroux, V., Sanchez, M., Carsin, A.-E., Schikowski, T., Adam, M., … Kauffmann, F. (2015). Ambient Air Pollution and Adult Asthma Incidence in Six European Cohorts (ESCAPE). *Environmental Health Perspectives*, *123*(6), 613–621. http://doi.org/10.1289/ehp.1408206

Jenerette, G. D., Harlan, S. L., Brazel, A., Jones, N., Larsen, L., & Stefanov, W. L. (2007). Regional relationships between surface temperature, vegetation, and human settlement in a rapidly urbanizing ecosystem. *Landscape Ecology*, *22*(3), 353–365. http://doi.org/10.1007/s10980-006-9032-z

Johnson, D. P., & Wilson, J. S. (2009). The socio-spatial dynamics of extreme urban heat events: The case of heat-related deaths in Philadelphia. *Applied Geography*, *29*(3), 419–434. http://doi.org/10.1016/j.apgeog.2008.11.004

Johnson, D. P., Wilson, J. S., & Luber, G. C. (2009). Socioeconomic indicators of heat-related health risk supplemented with remotely sensed data. *International Journal of Health Geographics, 8*(1), 57. http://doi.org/10.1186/1476-072X-8-57

Kalkstein, L. S., & Davis, R. E. (1989). Weather and Human Mortality: An Evaluation of Demographic and Interregional Responses in the United States. *Annals of the Association of American Geographers, 79*(1), 44–64. http://doi.org/10.1111/j.1467-8306.1989.tb00249.x

Lee, W. V. (2013). Historical global analysis of occurrences and human casualty of extreme temperature events (ETEs) - Springer. *Journal of the International Society for the Prevention and Mitigation of Natural Hazards*, *10*. http://doi.org/10.1007/s11069-013-0884-7

Lin, W., Yu, T., Chang, X., Wu, W., & Zhang, Y. (2015). Calculating cooling extents of green parks using remote sensing: Method and test. *Landscape and Urban Planning, 134*, 66–75. http://doi.org/10.1016/j.landurbplan.2014.10.012

Luber, G., & McGeehin, M. (2008). Climate Change and Extreme Heat Events. *American Journal of Preventive Medicine, 35*(5), 429–435. http://doi.org/10.1016/j.amepre.2008.08.021

Lundholm, J., MacIvor, J., MacDougall, Z., & Ranalli, M. (2010). Plant Species and Functional Group Combinations Affect Green Roof Ecosystem Functions. *PLOS ONE, 5*(3).

Miralles, D. G., Teuling, A. J., van Heerwaarden, C. C., & de Arellano, J. V.-G. (2014). Mega-heatwave temperatures due to combined soil desiccation and atmospheric heat accumulation. *Nature Geoscience, 7*(5), 345–349. http://doi.org/10.1038/NGEO2141

Mochizuki, T., Miyazaki, Y., Ono, K., Wada, R., Takahashi, Y., Saigusa, N., … Tani, A. (2015). Emissions of biogenic volatile organic compounds and subsequent formation of secondary organic aerosols in a Larix kaempferi forest. *Atmospheric Chemistry & Physics Discussions*, *15*(7), 10739–10771. http://doi.org/10.5194/acpd-15-10739-2015

Morgan, S., Celik, S., & Retzlaff, W. (2013). Green Roof Storm-Water Runoff Quantity and Quality. *Journal of Environmental Engineering*, *139*(4), 471–478. http://doi.org/10.1061/(ASCE)EE.1943-7870.0000589

Mueller, B., & Seneviratne, S. I. (2012). Hot days induced by precipitation deficits at the global scale. *Proceedings of the National Academy of Sciences*, *109*(31), 12398–12403. http://doi.org/10.1073/pnas.1204330109

Nardini, A., Andri, S., & Crasso, M. (2012). Influence of substrate depth and vegetation type on temperature and water runoff mitigation by extensive green roofs: shrubs versus herbaceous plants. *Urban Ecosystems*, *15*(3), 697–708. http://doi.org/10.1007/s11252-011-0220-5

Pachauri, R. K., Allen, M. R., Barros, V. R., Broome, J., Cramer, W., Christ, R., … others. (2014). Climate Change 2014: Synthesis Report. Contribution of Working Groups I, II and III to the Fifth Assessment Report of the Intergovernmental Panel on Climate Change. Retrieved from http://epic.awi.de/37530/

Pascal, M., Wagner, V., Le Tertre, A., Laaidi, K., Honore, C., Benichou, F., & Beaudeau, P. (2013). Definition of temperature thresholds: the example of the French heat wave warning system. *International Journal of Biometeorology*, *57*(1), 21–29. http://doi.org/10.1007/s00484-012-0530-1

Peng, L., & Jim, C. (2013). Green-Roof Effects on Neighborhood Microclimate and Human Thermal Sensation. *Energies*, *6*(2), 598–618. http://doi.org/10.3390/en6020598

Perini, K., & Magliocco, A. (2014). Effects of vegetation, urban density, building height, and atmospheric conditions on local temperatures and thermal comfort. *Urban Forestry & Urban Greening*, *13*(3), 495–506. http://doi.org/10.1016/j.ufug.2014.03.003

Polinsky, R. R. (2009). Evaluating the Effects of Green Roofs as Tools for Stormwater Management in an Urban Metropolis. Retrieved from http://scholarworks.gsu.edu/geosciences_theses/22/

Pompeii, W. C., & Hawkins, T. W. (2011). Assessing the impact of green roofs on urban heat island mitigation: a hardware scale modeling approach. *The Geographical Bulletin*, *52*(1), 52.

Qin, X., Wu, X., Chiew, Y.-M., & Li, Y. (2012). A Green roof test bed for stormwater management and reduction of urban heat island effect in Singapore. *British J. Environ. Climate Change*, *2*(4), 410–420.

Robinson, P. J. (2001). On the definition of a heat wave. *Journal of Applied Meteorology*, *40*(4), 762–775. http://doi.org/10.1175/1520-0450(2001)040<0762:OTDOAH>2.0.CO;2

Rosenfeld, A. H., Akbari, H., Romm, J. J., & Pomerantz, M. (1998). Cool communities: strategies for heat island mitigation and smog reduction. *Energy and Buildings*, *28*(1), 51–62. http://doi.org/10.1016/S0378-7788(97)00063-7

Rowe, D. B. (2011). Green roofs as a means of pollution abatement. *Environmental Pollution*, *159*(8-9), 2100–2110. http://doi.org/10.1016/j.envpol.2010.10.029

Saha, M. V., Davis, R. E., & Hondula, D. M. (2014). Mortality Displacement as a Function of Heat Event Strength in 7 US Cities. *American Journal of Epidemiology*, *179*(4), 467–474. http://doi.org/10.1093/aje/kwt264

Santamouris, M. (2014). Cooling the cities – A review of reflective and green roof mitigation technologies to fight heat island and improve comfort in urban environments. *Solar Energy*, *103*, 682–703. http://doi.org/10.1016/j.solener.2012.07.003

Sheridan, S. C., & Kalkstein, L. S. (2004). Progress in Heat Watch–Warning System Technology. *Bulletin of the American Meteorological Society*, *85*(12), 1931–1941. http://doi.org/10.1175/BAMS-85-12-1931

Smith, K. R., & Roebber, P. J. (2011). Green Roof Mitigation Potential for a Proxy Future Climate Scenario in Chicago, Illinois. *Journal of Applied Meteorology and Climatology*, *50*(3), 507–522. http://doi.org/10.1175/2010JAMC2337.1

Smith, T. T., Zaitchik, B. F., & Gohlke, J. M. (2013). Heat waves in the United States: definitions, patterns and trends. *Climatic Change*, *118*(3-4), 811–825. http://doi.org/10.1007/s10584-012-0659-2

Sobrino, J. A., Jiménez-Muñoz, J. C., & Paolini, L. (2004). Land surface temperature retrieval from LANDSAT TM 5. *Remote Sensing of Environment*, *90*(4), 434–440. http://doi.org/10.1016/j.rse.2004.02.003

Speak, A. F., Rothwell, J. J., Lindley, S. J., & Smith, C. L. (2012). Urban particulate pollution reduction by four species of green roof vegetation in a UK city. *Atmospheric Environment*, *61*, 283–293. http://doi.org/10.1016/j.atmosenv.2012.07.043

Steadman, R. G. (1979). The Assessment of Sultriness. Part II: Effects of Wind, Extra Radiation and Barometric Pressure on Apparent Temperature. *Journal of Applied Meteorology*, *18*(7), 874–885. http://doi.org/10.1175/1520-0450(1979)018<0874:TAOSPI>2.0.CO;2

Stone, B., & Rodgers, M. O. (2001). Urban form and thermal efficiency - How the design of cities influences the urban heat island effect. *Journal of the American Planning Association*, *67*(2), 186–198. http://doi.org/10.1080/01944360108976228

Stone, B., Vargo, J., Liu, P., Habeeb, D., DeLucia, A., Trail, M., … Russell, A. (2014). Avoided Heat-Related Mortality through Climate Adaptation Strategies in Three US Cities. *Plos One*, *9*(6), e100852. http://doi.org/10.1371/journal.pone.0100852

Stone, B., Vargo, J., Liu, P., Hu, Y., & Russell, A. (2013). Climate Change Adaptation Through Urban Heat Management in Atlanta, Georgia. *Environmental Science & Technology*, *47*(14), 7780–7786. http://doi.org/10.1021/es304352e

Targino, A. C., Krecl, P., & Coraiola, G. C. (2014). Effects of the large-scale atmospheric circulation on the onset and strength of urban heat islands: a case study. *Theoretical and Applied Climatology*, *117*(1-2), 73–87. http://doi.org/10.1007/s00704-013-0989-7

Thevenard, D. (2011). Methods for Estimating Heating and Cooling Degree-Days to Any Base Temperature. *ASHRAE Transactions*, *117*(1), 884.

U.S. Environmental Protection Agency Office of Atmospheric Programs. (2008). *Green Roofs* (Reducing Urban Heat Islands: Compendium of Strategies) (p. 29). Retrieved from http://www2.epa.gov/heat-islands/heat-island-compendium

Vautard, R., Yiou, P., D'Andrea, F., de Noblet, N., Viovy, N., Cassou, C., … Fan, Y. (2007). Summertime European heat and drought waves induced by wintertime Mediterranean rainfall deficit. *Geophysical Research Letters*, *34*(7). http://doi.org/10.1029/2006GL028001

Versini, P.-A., Ramier, D., Berthier, E., & de Gouvello, B. (2015). Assessment of the hydrological impacts of green roof; from building scale to basin scale. *Journal of Hydrology*, *524*, 562–575. http://doi.org/10.1016/j.jhydrol.2015.03.020

Vose, R. S., Karl, T. R., Easterling, D. R., Williams, C. N., & Menne, M. J. (2004). Climate (communication arising): Impact of land-use change on climate. *Nature*, *427*(6971), 213–214. http://doi.org/10.1038/427213b

Weng, Q. (2009). Thermal infrared remote sensing for urban climate and environmental studies: Methods, applications, and trends. *ISPRS Journal of Photogrammetry and Remote Sensing*, *64*(4), 335–344. http://doi.org/10.1016/j.isprsjprs.2009.03.007

Weng, Q., Lu, D., & Schubring, J. (2004). Estimation of land surface temperature–vegetation abundance relationship for urban heat island studies. *Remote Sensing of Environment*, *89*(4), 467–483. http://doi.org/10.1016/j.rse.2003.11.005

Yang, J., Yu, Q., & Gong, P. (2008). Quantifying air pollution removal by green roofs in Chicago. *Atmospheric Environment*, *42*, 7266–7273. http://doi.org/10.1016/j.atmosenv.2008.07.003

Yang, W., Wang, Z., Cui, J., Zhu, Z., & Zhao, X. (2015). Comparative study of the thermal performance of the novel green (planting) roofs against other existing roofs. *Sustainable Cities and Society*, *16*, 1–12. http://doi.org/10.1016/j.scs.2015.01.002

Yang, X., & Lo, C. P. (2002). Using a time series of satellite imagery to detect land use and land cover changes in the Atlanta, Georgia metropolitan area. *International Journal of Remote Sensing*, *23*(9), 1775–1798. http://doi.org/10.1080/01431160110075802

Zhang, Q., Miao, L., Wang, X., Liu, D., Zhu, L., Zhou, B., … Liu, J. (2015). Research Paper: The capacity of greening roof to reduce stormwater runoff and pollution. *Landscape and Urban Planning*. http://doi.org/10.1016/j.landurbplan.2015.08.017

APPENDICES

Appendix A

A series of conditional statements were needed to execute emissivity rasters in the ArcGIS raster calculator, including the creation of ‘masking rasters’ that effectively masked the zero values that resulted when using the ‘con’ function in the raster calculator.

NDVI_mask
Con(("NDVI" <= 0.5) & ("NDVI" >= 0.2), 1)

NDVI 0.2 – 0.5
"NDVI" * "NDVI_mask"

P*v* 0.2 – 0.5
("NDVI2to5" - 0.2) / 0.3 * ("NDVI2to5" - 0.2) / 0.3

Middle NDVI
0.004 * "Pv2to5" + 0.986

Low NDVI
Con(("NDVI" < 0.2), 0.973)

High NDVI
Con(("NDVI" > 0.5), 0.99)

Emissivity < 0.2
Con(IsNull("lowndvi"),0, "lowndvi")

Emissivity 0.2 – 0.5
Con(IsNull("middlendvi"),0, "middlendvi")

Emissivity > 0.5
Con(IsNull("highndvi"),0, "highndvi")

Final Emissivity Raster

If the emissivity has NODATA due to bands 3 and 4 having zero values, then use the following:

emiss2 = Con("emiss1" == 0, 0.973, "emiss1")